

IMPACT OF TOPOGRAPHY AND SPECIES DIVERSITY ON THE PREDICTION OF FOREST METRICS FROM VHR MULTISPECTRAL IMAGERY

MD SAROWAR HOSSAIN

July 2022

SUPERVISORS:

Dr. Ir. T.A. Groen

Dr. Ir. W. Bijker



IMPACT OF TOPOGRAPHY AND SPECIES DIVERSITY ON THE PREDICTION OF FOREST METRICS FROM VHR MULTISPECTRAL IMAGERY

MD SAROWAR HOSSAIN

Enschede, The Netherlands, July 2022

Thesis submitted to the Faculty of Geo-Information Science and Earth Observation of the University of Twente in partial fulfilment of the requirements for the degree of Master of Science in Geo-information Science and Earth Observation.

Specialization: Natural Resource Management (NRM)

SUPERVISORS:

Dr. Ir. T.A. Groen

Dr. Ir. W. Bijker

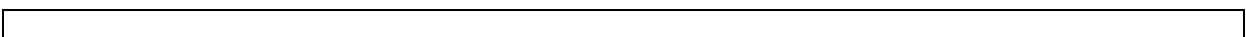
THESIS ASSESSMENT BOARD:

Dr. Ir. Anton Vrieling (Chair)

Dr.ir. M. Schelhaas (External Examiner, Wageningen University & Research)

DISCLAIMER

This document describes work undertaken as part of a programme of study at the Faculty of Geo-Information Science and Earth Observation of the University of Twente. All views and opinions expressed therein remain the sole responsibility of the author, and do not necessarily represent those of the faculty.



ABSTRACT

Multispectral remote sensing has been extensively used for estimation and monitoring of forest structural attributes. However, consideration of the influence of landscape factors such as topography and species diversity in forest attribute estimation are comparatively limited. To date, very few studies were found that evaluated the accuracy improvement of forest structure estimation models by incorporating topographic influence in the model and even fewer studies were found that investigated the changes in prediction accuracy by the influence of coniferous species diversity especially with multispectral imagery. Those studies that included topographic variables in their models, did not conclude how the topography effect the relations of other explanatory variables with forest attributes and whether or not that addition improved the model accuracy.

The aim of this study was to investigate: 1) how strongly the texture variables derived from VHR multispectral imagery correlate with forest metrics, which are mean diameter at breast height (DBH), standard deviation of diameter at breast height (SD DBH), and tree count per plot. 2) The changes in relationship between texture variables and forest metrics by the influence of slope and aspect and therefore any increase the models' estimation accuracy. 3) Any further improvement in models' estimation accuracy if the data is separated based on species diversity of the study area.

This study utilized the World View-2 derived texture variables calculated with different parameter settings to assess the relationship with field measured forest metrics. An iterative subsampling procedure was followed to fit stepwise regression models for each forest metric with the significantly correlated texture variables to determine the most significant variables and develop the prediction model, while the subsampling approach minimizes the spatial autocorrelation issue. Then, different models were developed adding slope, aspect, and their combined influence as interaction term in the stepwise prediction model running the subsampling algorithm and compared in terms of R^2 , RMSE and AICc. Moreover, the best fitted models were used to predict forest metrics in different species diversity forests.

The correlation coefficients of significant texture variables for Mean DBH ranged from -0.47 to -0.57, 0.36 to 0.41 for SD DBH and -0.51 to -0.56 for Tree Count. Interaction effect of slope and aspect on texture variables significantly changed the relationship with forest metrics in most cases and slope as a moderating variable, improved models' R^2 by 15%, 6%, and 11%, and the RMSE was decreased by 1.03, 0.54, and 0.3 for Mean DBH, SD DBH, and Tree Count, respectively. Aspect influenced model showed an increased R^2 by 4%, 5%, 5% and decreased RMSE by 0.29, 0.47, 0.17 for Mean DBH, SD DBH, and Tree Count, respectively. The best fitted models predicted Mean DBH, SD DBH and Tree count with an R^2 of 0.54, 0.45, and 0.42 and RMSE of 6.03, 3.86, and 3.73, respectively. Moreover, the splitting of model dataset based on species diversity showed that Mean DBH and Tree Count was predicted in single species forest stands with average R^2 of 0.60 and 0.50 and average RMSE of 5.70 and 3.48, respectively and SD DBH was predicted in multiple species forest stands with average R^2 of 0.68 and average RMSE of 2.80.

The correlation of texture variables with forest metrics was highly sensitive to GLCM parameter selection used to calculate the textures. The relationship of texture variables with forest measured variables changes significantly when texture variables have interaction effect of topographic variable. Therefore, forest structural attribute estimation accuracy can be improved in mountainous region by incorporating influence of topography and prediction can be even more improved if the model is fitted with species specific data.

Keywords: Forest metrics, World View-2, GLCM texture, Topographic influence, Rhodope Mountain, Species diversity, Spatial Autocorrelation, Subsampling algorithm, Interaction regression.

ACKNOWLEDGEMENTS

First of all, I would like to express my immense gratitude to the Faculty of Geoinformation Science and Earth Observation (ITC), the University of Twente, for considering me as an awardee of the ITC Excellence Scholarship to pursue my MSc degree.

Most importantly, I would like to acknowledge my deepest gratitude to my supervisor Thomas Groen for his cordial guidance from the beginning and for helping me in designing the whole research. I am deeply thankful to him for his valuable time, encouragement, and suggestions throughout the thesis phase. I would like to extend my earnest gratitude to my second supervisor Wietske Bijker for her critical comments which pushed me to sit back and rethink deeply.

I want to thank the 'Institute of Ecosystem and Biodiversity Research of the Bulgarian Academy of Sciences' for providing the field data. Special gratitude goes to Tzvetan Zlatanov for his suggestions and for providing insights about field data. He has been very friendly and reachable at any time. He also provided me the opportunity to carry out an internship at the above-mentioned organization which helped me in developing an understanding of the data I am using. I am thankful to European Space Agency (ESA) for providing me the imagery required for this study and also thanks to Petra Budde, Remote Sensing, and GIS Lab, Faculty ITC for helping me in obtaining WorldView-2 and WorldDEM DTM data from ESA.

I would like to acknowledge some good memories with my ITC friends from Bangladesh who gave me reasons to smile even on my toughest days. Last but not least, I want to take the time to thank my family members for their unconditional support in pursuing an MSc degree in a foreign country.

Md Sarowar Hossain
July 2022
Enschede, The Netherlands

TABLE OF CONTENTS

1.	Introduction.....	6
1.1.	Background.....	6
1.2.	Application of Remote Sensing to Estimate Forest Structural Metrics.....	6
1.3.	Review of Methods Used in Forest Structure Study.....	7
1.4.	Relation between image texture and forest structure.....	8
1.5.	Landscape Topography as an Influencing Factor of Forest Structure.....	9
1.6.	Sampling Design influence on Forest Structure Prediction.....	9
1.7.	Spectral Reflectance Variability as a Function of Species Diversity.....	10
1.8.	Research problem.....	10
1.9.	Research objectives.....	11
2.	Study Area and Data Description.....	13
2.1.	Study Area.....	13
2.2.	Data Description.....	13
3.	Methodology.....	17
3.1.	GLCM Texture Feature Selection.....	17
3.2.	Calculation of GLCM Texture Features.....	18
3.3.	Sensitivity Analysis of GLCM Parameter Selection.....	19
3.4.	Selection of Predictor Variables and Colinearity Assessment.....	19
3.5.	Assessment of Spatial Autocorrelation.....	19
3.6.	Subsampling of dataset and stepwise linear regression function.....	19
3.7.	Assessment of topographic variables influence on forest metrics prediction.....	20
3.8.	Assessment of Species Diversity Impact of Forest Metrics Prediction.....	21
4.	Results.....	22
4.1.	Determining the best combination of GLCM paramters.....	22
4.2.	Collinearity among texture variables.....	23
4.3.	Spatial dependency of data.....	24
4.4.	Correlation and Significance of Texture Variables with Forest Metrics.....	24
4.5.	Topographic Influence on Variable Relationship with Forest Metrics.....	26
4.6.	Performance of models for forest metrics prediction.....	28
4.7.	Species diversity influence on forest metrics prediction.....	30
5.	Discussion.....	34
5.1.	The importance of GLCM texture feature and their parameter selection in determining the relationship with Forest metrics.....	34
5.2.	Topographic effects in forest metric and image texture relationship.....	35
5.3.	Comparison of model prediction.....	35
5.4.	Prediction of forest metrics influenced by species diversity of stands.....	36
6.	Conclusion and recommendation.....	37
6.1.	Conclusions.....	37
6.2.	Potential application and Recommendations for future research.....	38

LIST OF FIGURES

Figure 2. 1: Map showing the location of study area and sampling points with a background of sentinel-2 natural color composite..... 13

Figure 2. 2: Sample field plots drawn from panchromatic band showing the variability in structure of forest stands. The samples are sorted by increasing plot mean DBH from left to right. 16

Figure 3. 1: Sequence of steps taken to achieve the research objectives..... 18

Figure 3. 2: sampling plots assigned to 500m grids. 20

Figure 4. 1: Correlation of texture features with different parameter settings and Mean DBH. a) NDVI Homogeneity with varying window sizes and orientations, b) NDVI Homogeneity with varying displacement length and orientations, c) Pan Cntr with varying window sizes and orientations, and d) Pan Cntr with varying displacement length and orientations. 22

Figure 4. 2: Plots showing a) correlation among texture variables and b) VIF values..... 24

Figure 4. 3: Semi variogram model showing the range of spatial dependence around neighbouring pixels of a) Nir-1 b) NDVI c) Panchromatic bands. 24

Figure 4. 4: Variable significance plot showing the texture variables selected for forest metrics a) Mean DBH, b) SD DBH, c) Tree Count; and the number of times they became significant at $\alpha = 0.01$ and 0.05 26

Figure 4. 5: Variable significance plot for Mean DBH a) Model_{Slope} b) Model_{ASP} c) Model_{Com}, showing the number of times the variables were included in the model and became significant at $\alpha = 0.01$ and 0.05 . .. 28

Figure 4. 6: Boxplots showing the R², RMSE and AICc distribution for Mean DBH (a,d,g); the R², RMSE and AICc distribution for SD DBH (b,e,h); and the R², RMSE and AICc distribution for Tree Count (c,f,i). 29

Figure 4. 7: Field measured forest metrics vs. predicted forest metrics values from best fitted models a) Mean DBH Model_{Slope}, b) SD DBH Model_{Com}, c) Tree Count Model_{Slope}. Predicted values are the average from 100 different models. 30

Figure 4. 8: Boxplot summaries of the forest metrics and image texture characteristics in single species and multiple species forest plots..... 31

Figure 4. 9: Scatterplots of predicted vs. observed a) Mean DBH, b) SD DBH, c) Tree count in single species and multiple species plots. 32

Figure 5. 1: Predicted vs. observed Mean DBH values from the model fitted with panchromatic contrast and blue entropy texture having the interaction effect of slope..... 36

LIST OF TABLES

Table 2. 1: Summary statistics of forest metrics.	14
Table 2. 2: Output of georectification process showing average positional error remote sensing images. .	15
Table 3. 1: Description of GLCM texture features used in this study.	17
Table 3. 2: GLCM parameter used for texture extraction.....	18
Table 4. 1: Pearson correlation coefficients between forest metrics (Mean DBH, SD DBH, Tree Count) and selected texture variables. (W = window size, D = displacement length and O = orientation).....	25
Table 4. 2: Texture variables selected for developing Model _{Base}	26
Table 4. 3: Coefficients of regression and p-values for variables from four different models of Mean DBH, SD DBH, and Tree Count. Values indicate average of 100 iterations of the models following the subsampling of dataset.....	27
Table 4. 4: Average and standard deviation of R ² and RMSE values of Mean DBH, SD DBH, and Tree Count in single species and multiple species plots (n = 59). The t statistics indicate the differences in the predicted values of forest metrics.	33

1. INTRODUCTION

1.1. Background

Forests are a prominent kind of ecosystem in Europe, accounting for 42 percent of the land area (Ganault et al., 2021) and delivering a variety of important ecosystem services such as timber stocks, carbon sequestration, habitat for biodiversity, and watershed protection (Scherer-Lorenzen & Schulze, 2005). These services are heavily reliant on forest species richness as well as other characteristics of structural attributes (e.g., tree density and volume) in a forest ecosystem (Gamfeldt et al., 2013). Hence, forest structural attributes are critical components of ecosystem, and are connected to a variety of ecological phenomena (Pretzsch, 2009; Shugart et al., 2010). The monitoring and estimation of these attributes of forest are important for sustainable use of forest in multiple ways, such as increasing productivity, habitat, and biodiversity conservation (Freitas et al., 2005).

Forest structure can be described by several attributes, including canopy cover, basal area, tree height, leaf area index, stem volume, diameter at breast height (DBH), tree species mixture, biomass, and spatial arrangement (horizontal and vertical) of vegetation (Ozdemir & Karnieli, 2011). Among several structural attributes, a few attributes such as DBH, number of trees per unit area are important as they provide information about some critical characteristics of forest stand (Goff & Zedler, 1968). Metrics of DBH such as Mean DBH and standard deviation of DBH (SD DBH) are usually used as a measure of stem diameter distribution of forest stand and diameter variability within the forest (Zenner and Hibbs, 2000). In addition, tree count per unit area is an important structural attribute to understand how dense the forest stand is. For forest management, it is critical to have this information to better understand the management needs. For instance, thinning of dense forest stands may enhance diameter development (Baldwin et al., 2000; Fuhr et al., 2001).

1.2. Application of Remote Sensing to Estimate Forest Structural Metrics

Detailed and accurate estimation of forest attributes is necessary for forest inventory and management, growing stock, biomass, biodiversity, and carbon modelling (R. Zhou et al., 2019). Conventional field surveys offer trustworthy forest attribute data which can be used to monitor and manage forests (Scrinzi et al., 2007), but most of the time they are labour-intensive, costly, and difficult to deploy, especially in hilly and remote forest locations (R. Zhou et al., 2018). The ability to accurately estimate forest structural attributes on a large area from tree size measurements is a focal concern in forest inventory (Hall et al., 2011). Remote sensing appears to be a viable and low-cost approach for evaluating forest biophysical attributes compared to field surveys, when the area is large or difficult to reach. In DBH estimation and tree density mapping study, a number of remote sensors have been employed, including LiDAR (Huang et al., 2011; Wu et al., 2015; Xie et al., 2020; Yao et al., 2012), aerial synthetic aperture radar (SAR) (Hyypä et al., 2000; Karjalainen et al., 2012), optical airborne data (Lévesque & King, 2003; Pasher & King, 2010; Tuominen & Pekkarinen, 2005), and optical satellite hyperspectral- (Cho et al., 2009) and multispectral imagery (Beguet et al., 2014; Ozdemir & Karnieli, 2011; Vázquez De La Cueva et al., 2008; Wunderle et al., 2007). In particular, LiDAR remote sensing has become as a convenient tool for predicting such forest attributes. Naesset (2007) observed that predictions of forest attributes including tree height, DBH, tree density, volume, and basal area obtained from models developed utilizing LiDAR data did not significantly differ from field measured data, indicating its effective use in forest inventory. However, the high expense of large-area applications requiring frequent revisits limits its applicability (Wolter et al., 2009). Recent advances in SAR technology supports its application in large-area forest inventory. Though SAR images provide a reasonable estimation of forest structures, Hyypä et al. (2000) concluded that radar images contain less information for forest inventory than optical imagery, and the estimation capability of SAR is

very much site-specific. They found that some spectral information from NIR and SWIR bands are more useful in characterizing forest attributes. Unlike Radar and LiDAR, multispectral satellite imagery has some advantages in estimating forest attributes, including its extensive temporal and spatial coverage and simple interpretation relying on traditional photographic image analysis.

In the last few decades, optical remote sensing data has been thoroughly tested and used to identify spatial patterns in canopy surfaces for estimating different forest attributes (Lamonaca et al., 2008; Wolter et al., 2009). However, predictions from moderate resolution sensors do not provide sufficient accuracy needed to capture structural attributes for forest management (Helmer et al., 2012; Pierce et al., 2009). Hyypä et al. (2000) examined the accuracy of obtaining the following stand variables: stem volume, mean basal area, and tree height, using several image sources such as aerial pictures, SPOT XS, SPOT Pan and Landsat TM and concluded that the accuracy obtained ranked according to their spatial resolution. In this regard, incorporation of very high resolution (VHR) images with information from other sources (such as forest inventory and GIS data) was found useful for drawing fine-grained assessments of forest structural attributes and for strengthening the abilities of investigating the forest ecosystem (Kayitakire et al., 2006; Leboeuf et al., 2007; Nyamgeroh et al., 2018; M. A. Wulder et al., 2004).

1.3. Review of Methods Used in Forest Structure Study

Using optical imagery, radiative transfer and empirical models are two broad techniques in forest structure modeling. Because of radiative transfer models mainly relies on spectral information (Leblanc, 1998; Peddle et al., 2004), they are not capable of utilizing spatial information (Bruniquel-Pinel & Gastellu-Etchegorry, 1998) In contrast, empirical investigations are more used in forest attribute modelling, since it can utilize image spectral information, but also image spatial details in forms of image texture (Nyamgeroh et al., 2018; Tuominen & Pekkarinen, 2005; Wood et al., 2012), spatial dependency measures like semi-variance (Johansen & Phinn, 2014; Treitz & Howarth, 2000), radiometric fraction at the pixel level (spectral unmixing), or a combination of these (Lévesque & King, 2003b) . Still, direct measurement of DBH using passive remote sensing data is thus tricky since trees grow mostly vertically and the top components of the tree, especially branches and canopy cover, often conceal the direct view of the stem (Kattenborn et al., 2018; Kayitakire et al., 2006; Ozdemir & Karnieli, 2011). However, multispectral optical data-derived spectral bands, indices, and textures indirectly relate to DBH through the crown diameter (Cho et al., 2009). In remote sensing of forest parameters, the most often utilized texture measures are a set of the second-order statistics of spectral value, popularly known as Grey Level Co-occurrence Matrix (GLCM) developed by Haralick et al. (1973). The advantage of using GLCMs are their ability to carry details about the spectral intensity of pixels and neighboring pixels (Tuttle et al., 2006). However, their application in forests is tricky because of their performance depends on various parameter settings. In addition to texture measures, vegetation indices (VIs) can capture the spectral response of canopy structures using their relationship with leaf area index (LAI) or crown cover (Ingram et al., 2005), since the canopy structure is shaped by vegetation parameters such as height, density, age, basal area, etc. (Peterson et al., 1987; Rock et al., 1986) . There are many VIs though NDVI is most used in forest parameter estimation studies (Cho et al., 2009; Ingram et al., 2005; Kayitakire et al., 2006; Ozdemir & Karnieli, 2011), since it has been shown theoretically and experimentally to be related with canopy cover (Pau et al., 2012). However, NDVI is not sensitive to higher biomass levels which is one of the drawbacks of this index in tropical forests (Ingram et al., 2005). Townsend (2002) found that adding NDVI as a variable with SAR data improves the model prediction of basal area in the forest.

In addition, forest structure prediction mostly depends on regression models established on empirical relationship between ground measured information and corresponding remote sensing data. The statistical

procedure of prediction can often be biased by uncertainties like multicollinearity and spatial autocorrelation (Rocha et al., 2019; Shiklomanov et al., 2016). In regression models, the key issue is to minimize the multicollinearity of the spectral and textural variables to build stable models and prevent overfitting (Beguet et al., 2012). Variance inflation factor (VIF), a powerful multicollinearity indicator (Alin, 2010), can be used to address this issue. Spatial autocorrelation also performs an essential role in selecting environmental factors and further affects forest attribute prediction (Liu et al., 2018). Autocorrelation within variables triggers multicollinearity, increasing the probability that critical variables are not identified (type II error). In contrast, a violation of the assumption of data independency and equally disseminated observations raise the risk of a type I error (Babcock et al., 2013; Dormann et al., 2013; Fortin et al., 2012). Most of the existing model evaluation technique focuses primarily on model fit and improving accuracy while giving very little consideration to the effects of spatial autocorrelation on variable choice, and its influence on predictions remains unambiguous (Moisen & Frescino, 2002; Rocha et al., 2019; Zhang et al., 2005) In forest structure research, evaluating the influence of sampling density and its induced spatial dependence in variables may increase the reliability of model prediction (Dupuy et al., 2012).

1.4. Relation between image texture and forest structure

In recent times, texture features from high-resolution imagery have shown their ability to estimate vegetation structures such as tree DBH with considerable accuracy, while spectral information of optical imagery or air photographs cannot measure them directly (Ozdemir & Karnieli, 2011; Wood et al., 2012; J. Zhou et al., 2017). Image texture has been employed in many studies to estimate forest biomass, DBH distribution, tree density, and height differences in both broadleaf and coniferous forests (Beguet et al., 2014; Ingram et al., 2005; Kayitakire et al., 2006; Wunderle et al., 2007). Texture analysis measures the variation in tonal values of pixels within a specified area of an image (Wood et al., 2012), which was found useful in detecting objects or region of interests (Pope & Treitz, 2013). Zhao et al. (2018) demonstrated that textural analysis of image is more useful than spectral information for estimating attributes that is related to vegetation canopy. Ozdemir & Karnieli (2011) showed that mean and standard deviation of DBH and number of trees can be estimated with high accuracy in a coniferous plantation forest using texture analysis of World View-2 image. Hence, it is obvious that the textural information obtained from high-resolution satellite images is valuable for measuring forest stand density and diameter distribution.

Image texture is a sophisticated metric, and texture values determined with the GLCM technique are very sensitive to window size, orientation, displacement length, and physiographic settings (Coburn & Roberts, 2010; Kayitakire et al., 2006; Sarker & Nichol, 2011). Kayitakire et al. (2006) showed that for prediction of structural attributes in a conifer forest, the most important GLCM parameters were window size, displacement length and orientation. However, it remains confusing of specific parameter settings for window size, displacement length and orientations when calculating GLCM textures (Zhou et al., 2017). For instance, there are different recommendations about whether to select a large or small moving window size. Some investigations have demonstrated that image texture measures estimated using a small window size from high resolution images are most significantly related with observed vegetation structure on the field (Wood et al., 2012; Wunderle et al., 2007). Others found that smaller window sizes contributed to the poor correlation of GLCM textures with forest structural attributes (Franklin et al., 2010). (Coburn & Roberts, 2010) showed that texture features cannot be expressed precisely with a single moving window size and when the investigated forest surface is homogenous, a small window size can be used.

Displacement length is another crucial factor that influences the value of GLCM textures. Low comparability is caused by a large pixel displacement. However, few studies have looked at how displacement length effects texture features. Kayitakire et al. (2006) found that displacement lengths effects

on GLCM texture can be more related to the characteristics of forest and image spatial resolution. They also found that orientation had little influence on the estimation accuracy of forest attributes. However, Clausi (2014) proposed that each orientation should be evaluated to obtain best result from GLCM texture. Zhou et al. (2017) mentioned about the average value of texture from four orientation, however, no specific findings reported the effect of average orientation in forest structure estimation. Therefore, the determination of optimal moving window size, displacement length and orientation for highest correlation of textures with forest attributes needs further analysis.

1.5. Landscape Topography as an Influencing Factor of Forest Structure

Topographic features such as altitude, slope, and aspect are major drivers of forest structure and composition as it regulates the distribution of trees in a forest, hydrologic processes, soil chemistry and microclimate (Gallardo-Cruz et al., 2009; Yeakley & Weishampel, 2000). Altitude and aspect play a consequential role in determining the temperature regime and atmospheric pressure of any geographical area (Singh et al., 2016). For species found in higher altitudes, ridges and steep slopes, strong competition for essential nutrients and water is crucial to their long-term survival (Heineman et al., 2011; Paoli et al., 2008). On the other hand, in alluvial valleys, forests tend to face intense competition for the light which allows them to grow taller and stratified canopies (Banin et al., 2012; Paoli et al., 2008; Werner & Homeier, 2015) as well as enhances their productivity and turnover rate (Aiba et al., 2005; Jucker et al., 2018).

Eilu & Obua (2005) reported that variation in altitudes and slopes in a forest can cause variation in the species richness and their dispersion behavior. In addition, Kharkwal et al. (2005) have underpinned altitude and climatic factors (i.e temperature and rainfall) as the key determinants of species richness. Moreover, forest landscape structure and species association are greatly impacted by topographic factors (Behera et al., 2006).

In forest lands, both the energy and water balance conditions are highly induced by the patterns of solar radiation. At mid and high latitudes, slopes facing the Equator are warmer than slopes facing the closest pole since the former receive more radiation. Therefore, in the northern hemisphere, the south slopes tend to provide the most suitable habitat for organisms with the southern distribution. While for organisms with northern distribution, north slopes are considered to be the ideal habitat (Stoutjesdijk & Barkman, 2014).

Apart from affecting vegetation attributes, topographic features influence remote sensing analyses by changing the radiance of the images as the incidence and exitance angles change with varying slope aspects and altitude (Huang et al., 2008). The reflectance is controlled by sun-terrain-sensor geometry. In mountainous forests, the geometry can vary between pixels and eventually may result in spectral variations (Tan et al., 2013). The illumination effect and self-shadowing are common to hilly and coniferous forests. For instance, topographic deviations can intensify the difficulty of classifying stand complexity through mimicking canopy complexity (Kane et al., 2008). While, steep slopes generate shades that minimize the variation in vegetation cover during image classification (Holmgren & Thuresson, 2008).

1.6. Sampling Design influence on Forest Structure Prediction

Sampling design serves as an integral part of empirical modeling with spatial data (Næsset et al., 2015; Ozdemir & Karnieli, 2011). Inappropriate sampling design particularly the plot design can affect the association between remote sensing data and forest structure parameters by forest edge effect and co-registration errors (Ruiz et al., 2014). Often larger plot sizes are considered more advantageous for remote sensing-assisted estimation as they tend to capture more of the variability in the forest population (Næsset et al., 2015), maintain a higher degree of spatial overlap of tree canopies in a forest stand (Frazer et al., 2011). Ene et al. (2007) analyzed the effect of the plot size on forest inventory by considering 3 different plot sizes (200, 400 and 600 sq meter). Similarly, Gobakken & Næsset (2009) carried out a comparative study on the

effect of plot areas of 200 sq meters and 300 sq meters. Further Frazer et al. (2011), analyzed the plot area co-registration effect for the estimation of biomass using circular plots with four different radii (10, 15, 20, 25 m) and 25*25m square shaped plots. Mascaro et al. (2011) quantified this effect for tropical sample plots of different sizes. It was evident from all the above-mentioned forest structure attribute estimation studies that the larger plot areas provide higher accuracy and minimize plot boundary effects and co-registration errors. Besides, (Næsset et al., 2015) considered the effects of geometric shape of plot on forest feature modeling and pointed out that circular plots are more favorable than rectangular plot in terms of acquisition of accuracy. However, larger plot sizes incur high economic cost of field work; therefore, in order to obtain optimal modelling performance, combining plot boundary and density of remote sensing data can be a viable option (Ruiz et al., 2014).

1.7. Spectral Reflectance Variability as a Function of Species Diversity

Species diversity is an important attribute of forest ecosystem and is related to the biophysical structure of the forest (Guisasola et al., 2015). Lähde et al. (1999) mentioned that species diversity and stand structure of the forest both can influence each other in a forest ecosystem. The presence of many species in a forest stand may alter the dimensions of various tree compartments including the stem, branches, and foliage (Barbeito et al., 2017; Pretzsch, 2014) and such changes may result in an increase in the crown size and shape variability of a particular species in mixed stands. Variations in crown structure have an effect on the spectrum response acquired by remote sensing imaging; however, the spectral response varies depending on the spatial and spectral resolution of the sensor (White et al., 2010). Previous studies carried on mixed forests using remote sensing approach mentioned that estimation of forest attributes is difficult in mixed forest due to complex canopy structure compared to single species stands (Ma et al., 2017; St-Onge et al., 2008). Heurich & Thoma (2008) found a 24% improvement in DBH estimation model accuracy when stands of coniferous species were modelled separately from mixed species stands with airborne lidar data. The studies found comparing the prediction of forest structural attributes based on species diversity, they employed segregation of coniferous species from the broadleaf species in mixed forest. Therefore, a knowledge gap exists on how forest stands with multiple coniferous species influence the accuracy of forest structure estimation in comparison to forest stands with a single species.

1.8. Research problem

A fundamental goal of forest resource assessment is to estimate the forests' growth, growing stock, and overall health (Hyyppä et al., 2000). To characterize the forest growth and condition, accurate prediction of structure attributes is essential. However, most of the recent studies intended to predict forest structural attributes utilizing VHR multispectral imageries have shown a varying level of accuracy (Castillo-Santiago et al., 2010; Kayitakire et al., 2006; Ozdemir & Karnieli, 2011). As a reason, Salvador and Pons (1998) mentioned that forest type and environment of study location significantly influence the functional links between forest attributes and information gained from imagery. They also found that the relations are even more varied with heterogeneous ecosystems that have scattered forest stands.

Therefore, due to variation in several environmental considerations, such as topography, relative location, aspect, water availability and soil composition, precise estimation of forest structural characteristics with remote sensing data is difficult to determine (Sabol et al., 2002; Urquiza-Haas et al., 2007). When the study site landscape is topographically heterogeneous, huge variation occurs in forest structure with major uncertainties in the estimation of structural attributes (Houghton et al., 2001; Saatchi et al., 2007). According to Brososke et al. (2014), accurate estimation of structural attributes is quite challenging in complex forests and the addition of ancillary information such as climate and topography might help to mitigate this issue. Many studies tried to understand the function of ecosystem aspects that influence spatial distribution and variation of forest structure (Avolio et al., 2015; Saatchi et al., 2007). Yet, the impact of large (more than

2000 m range) altitude fluctuation on structural attributes has not been properly understood (Leuschner et al., 2007; Zach et al., 2010). Moreover, several studies tried to evaluate the influence of topography on estimation accuracy of forest structural attributes by segmenting the forest based on altitude, slope, and aspects classes (Donoso et al., 2007; Leitold et al., 2014; Pasher & King, 2010). However, when corrected by topographic variables, the changes in remote sensing variable significance and subsequent increase in estimation accuracy of forest structural attributes still needs to be investigated.

In addition to topographic variation, prediction of forest structural parameters more challenging in species diverse forests than in homogenous forests (Broszofske et al., 2014). Several studies mentioned about the differences in spectral response of forest because of species composition (Ozdemir & Karnieli, 2011; Pühr & Donoghue, 2010; Wolter et al., 2009). White et al. (2010) found that species diverse forest stands tend to have a weak spectral response, while plantations and coniferous forests of single species have shown a very good result in prediction of structure parameters. According to findings some researchers have suggested that categorizing survey plots based on species might increase the accuracy of model prediction (Olsson, 1994; Peterson et al., 1986).

For this study, an old growth natural forest has been chosen located in Rhodope Mountain. The terrain of this forest is highly heterogenous with moderate to steep slopes. Most of the forest area is dominated by coniferous trees with sparsely distributed broadleaf trees. This forest falls under the birds and habitat regulation by Natura 2000 since Bulgaria joined to European union in 2007. However, there is no study or project undertaken to understand the spatial distribution of compositional and structural diversity of the forest (Nyamgeroh et al., 2018). This study will investigate the capability of multispectral remote sensing to predict forest metrics in relation to landscape topography. This study will also compare the prediction capability in forest stands with different species diversity condition. This study may provide an understanding about the importance of topographic features and species diversity to be considered in forest structure prediction models. This information will be useful for future forest structure studies in linking remote sensing models with landscape factors.

1.9. Research objectives

1.9.1. General objective

The overall objective of this study is to evaluate how topography and species diversity influence the estimation of forest structural metrics from VHR multispectral imagery in a central European forest.

1.9.2. Specific objectives and questions

1. To determine the strength of the relationship between three forest structural metrics (Mean DBH, SD DBH and Tree Count) and image variables (GLCM textures from spectral bands and vegetation indices).

- Which image variables correlate significantly (at $\alpha = 0.05$) with forest structural metrics?

2. To assess the influence of topographic variables (slope and exposure) and species diversity classes on the relationship between forest structure metrics and multispectral image variables.

- Do the regression coefficients of significant predictor variables change considerably by correcting for Slope?
- Do the regression coefficients of significant predictor variables change considerably by correcting for Aspect?
- Are the relations between image variables and forest structural metrics stronger (in terms of R^2 and RMSE) in plots with single species than in plots that consist of multiple species?

1.9.3. Research Hypothesis

- H1: The GLCM textures with plot level window size (15.98m diameter) having smaller displacement lengths ($\leq 3.2\text{m}$) and average orientation are significant predictor (at $\alpha = 0.05$) of forest structural metrics in Rodophe Forest.
- H1: At flatter slopes, relationships between forest structure metrics and image-based variables are stronger than at steeper slopes.
- H1: At southward aspect, relationships between forest structure metrics and image-based variables are stronger than in northward aspect.
- H1: Single species plots produce higher R^2 and lower RMSE than multiple overstory tree species plots from the relationship between Forest stand metrics and remote sensing variables.

2. STUDY AREA AND DATA DESCRIPTION

2.1. Study Area

The study area is located in the Rhodope Mountain range, near the city of Smolyan in Bulgaria. The extent of the area lies between (41°38'9" N, 24°35'56" E) and (41°35'36" N, 24°39'23" E) and covers an area of about 2150 ha (fig. 2.1). This area of the Rhodope Mountain range is a part of Natura 2000 regulation, which is part of the European Union's nature protection program. The topography of the location is mountainous, and the altitude varies between 1180 to 2125m.

The forest on the Rhodope range is a natural forest and tree species comprises several conifer populations. Common coniferous species of the forest are *Picea abies* (Norway spruce), *Abies alba* (Silver fir), *Pinus sylvestris* (Scot's pine) and broadleaf trees are *Sorbus aucuparia* (European mountain-ash), *Fagus sylvatica* (European beech), *Corylus avellana* (Common hazel). Although, *Picea abies* is the most dominant species in the study location. These species are mainly distributed in the altitudinal range between 1200m to 1850m above sea level in the study area (Zlatanov et al., 2017).

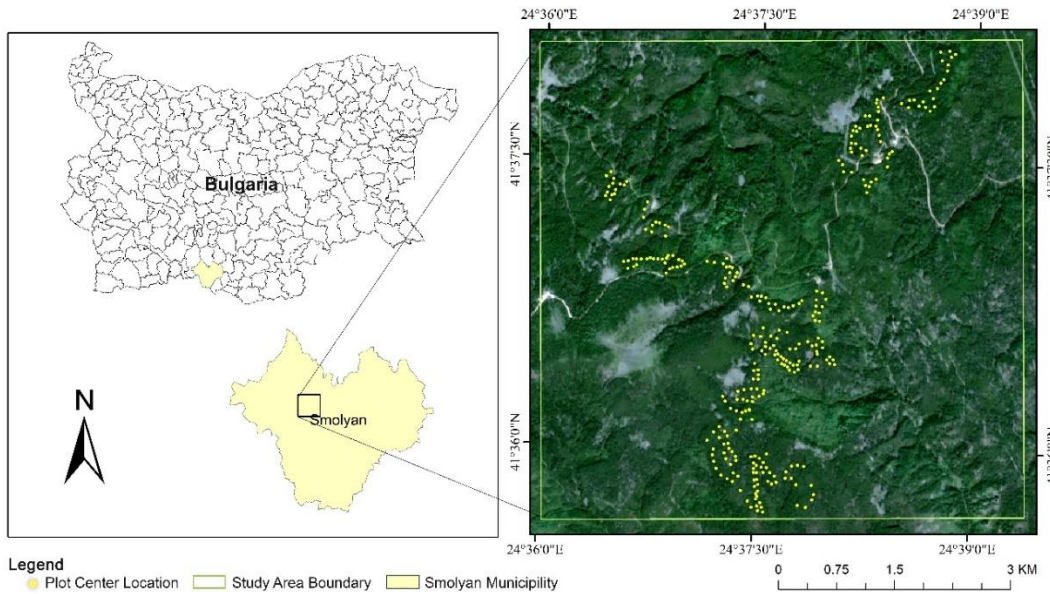


Figure 2. 1: Map showing the location of study area and sampling points with a background of sentinel-2 natural color composite.

2.2. Data Description

2.2.1. Description and processing of field data

The field measured data for this study was obtained by the Institute of Ecosystem and Biodiversity Research of the Bulgarian Academy of Sciences. The data was collected during the summer of 2020 and consists of 320 circular sampling plots. The selection of sampling plots was random and targeted to capture the spatial distribution of conifer forest species. Each of the circular sampling plot were 7.98m in radius having an area of 200 m². The average distance between the centers of field plots was about 45m.

Six forest stand and individual tree variables were collected, which describes the forest stand characteristics of each plot. The procedure for measurements of the plot data is described by Nikolov et al. (2022). The collected variables were: 1) Individual tree DBH in 4cm width DBH classes. 2) Number of species per plot,

3) Tree count per plot, 4) Canopy cover in percent, 5) Tree Height (cm) in four height classes, 6) Volume of dead wood per plot.

From the obtained data, four forest metrics were calculated which were Mean DBH, SD DBH, Tree Count per plot and Shannon Diversity Index. The metric of Mean and SD DBH (Eq. 1 and 2) was calculated by averaging individual tree data and estimating deviation of each tree DBH from the mean. Shannon's diversity index, developed by Shannon (1948), was calculated as an indicator of species diversity from number of species data (Eq. 3). Tree count was entered in the dataset as a metric of tree number per plot in the field.

Mean DBH

$$= \frac{\sum_{i=1}^n d_i}{n} \quad (1)$$

SD of DBH

$$= \sqrt{\frac{\sum_{i=1}^n (d_i - \bar{d})^2}{n - 1}} \quad (2)$$

In eq. 1 and 2, d_i represents diameter of tree stems and \bar{d} indicates the mean of DBH from n number trees.

$$SDI = \sum p_i \ln p_i \quad (3)$$

Where, p_i is the ratio of number of individual trees of the i th species.

While calculating the metrics, trees with DBH less than 10 cm were eliminated from the calculation, Since trees having smaller DBH are mostly not in the canopy and we are looking at forest metrics from multispectral remote sensing that is more related to the open canopy area of trees. A summary statistic of the metrics is given in table 2.1.

Table 2. 1:Summary statistics of forest metrics.

	Mean DBH (cm)	SD of DBH (cm)	Tree No. per plot	Shannon's Index
Min	10.00	0.00	2	0.00
Max	67.00	37.74	27	0.96
Mean	33.90	11.44	9.41	0.09
Std deviation	10.11	5.99	4.86	0.21

2.2.2. Remote Sensing Data

2.2.2.1. Very High-Resolution World View 2 Imagery

A WorldView-2 multispectral imagery, acquired on 21 June 2021 was used in this study. The imagery was chosen based on the criteria of cloud cover and nadir angle. The selected WorldView-2 image has a 0.5% cloud cover over the area and was captured at a 11-degree nadir angle. Moreover, during the image capture the sun azimuth angle was 166.8 degree, and the sensor was in forward direction having an azimuth angle of 21.5 degree. Seed & King (2014) demonstrated considerable negative effects of viewing angle greater than 10-degrees on forest structure modeling. This study initiated with the analysis of a Geo-Eye satellite imagery having a nadir angle of 25.6 degrees, which yielded a very poor correlation coefficients with field measured

metrics. Therefore, it was important to look for an imagery with properties appropriate for forest structure modelling.

The imagery comprises eight spectral bands with a spatial resolution of 1.6m and one panchromatic band of 0.44m spatial resolution. The spectral range of multispectral bands are between 400-450 nm (Coastal Blue), 450-510nm (Blue), 510-580nm (Green), 585-625nm (Yellow), 630-690nm (Red), 705-745nm (Red Edge), 770-895nm (Nir-1), 860-1040nm (Nir-2) and 450-800nm for the panchromatic band.

The imagery was obtained as an Ortho Ready Standard (OR2A) product, which was radiometrically, and sensor corrected (DigitalGlobe, 2010). Therefore, the pre-processing of the imagery includes orthometric correction and georectification. The orthometric correction was done to reduce the distortions on the imagery influenced by heterogenous terrain and was carried out using the WorldDEM DTM data as topographic reference. The georectification was carried out using the Auto Sync Workstation tool in Erdas Imagine. The reference image used for georectification was a UAV imagery of the study area. The AutoSync tool finds identical points from both images and calculates the positional error in input imagery from the reference image. A total of 161 and 83 identical points were chosen which has a RMSE less than 1m respectively for multispectral and panchromatic image for georectification. Finally, the average positional error found in multispectral and panchromatic image were 0.596 m and 0.682 m respectively (table 2.2)

Table 2. 2: Output of georectification process showing average positional error remote sensing images.

Bands	No. of GCPs	Avg. X residuals	Avg. Y residuals	Avg. RMS Error (m)
Multispectral	161	-0.021	0.004	0.596
Pan	83	0.025	-0.063	0.682

From the corrected Nir-1 and Red spectral bands NDVI was calculated (Eq. 4) as an indicator of tree canopy characteristics.

$$NDVI = (Nir1 - Red) \div (Nir1 + Red) \tag{4}$$

The sample panchromatic images in Fig. 2.2 demonstrates the variation in canopy structure among measured field plots. The field measured plots cover a 100 m² circular area on the multispectral and panchromatic bands where the horizontal width of field plots is 35 pixels and 9 pixels in the panchromatic and multispectral band, respectively.

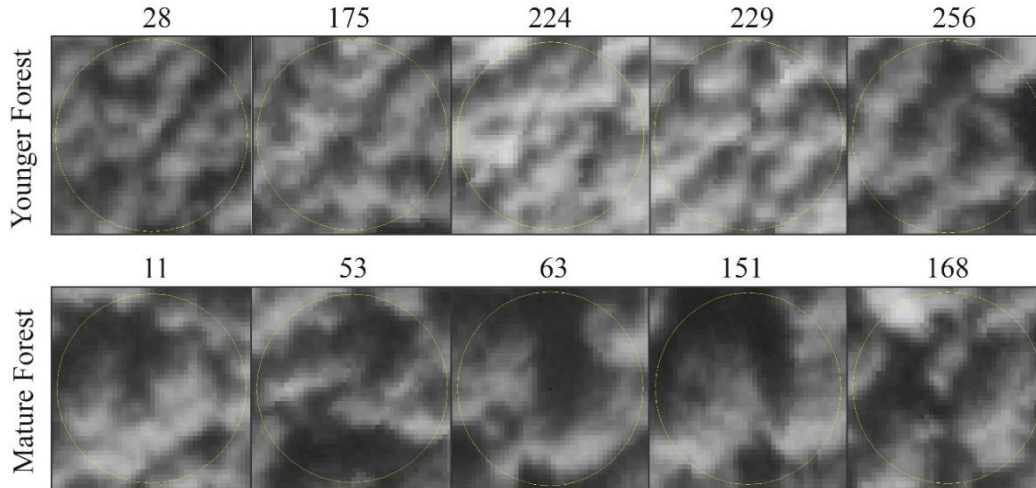


Figure 2. 2: Sample field plots drawn from panchromatic band showing the variability in structure of forest stands. The samples are sorted by increasing plot mean DBH from left to right.

2.2.2.2. WorldDEM DTM Data

To explore the influence of landscape topography on prediction of forest metrics, we obtained a Digital Terrain Model (DTM), captured on 2014 from the TanDEM-X mission. The obtained WorldDEM DTM has a spatial resolution of 12m, and relative vertical accuracy is less than 2m (slope $\leq 20\%$) (AIRBUS, 2020). The topographic variables extracted from the DTM were Elevation, Slope and Aspect. Since, the altitude of our sampling plots does not vary significantly, we excluded further analysis of altitude in our study. Slope values were calculated from the DTM in degree unit. In addition, the aspect calculated from DTM was standardized to a linear scale of 0 to 1 to normalize the direction from north to south, where 0 represents 22.5° NNE and 1 represents 202.5° SSW. Eq. 5 shows calculation used to standardize the aspect. Since forest stands respond differently towards north and south directions, the standardization of aspects from north to south facilitates establishing a linear relationship with forest metrics.

$$Aspect = \frac{(ABS(180 - ABS(202.5 - Aspect)))}{180} \quad (5)$$

Where, *ABS* represents the absolute of values.

3. METHODOLOGY

3.1. GLCM Texture Feature Selection

GLCM is a descriptor, that is used to extract spatial variation and texture statistics through incorporating co-occurrence probability matrix (Haralick, 1979), where each value of the matrix represents the probability of nearest neighbour grey tone at a given distance and orientation (J. Zhou et al., 2017). From the 14 texture features described by Haralick et al. (1973), we selected 6 second order texture features (table 3.1) based on their frequent use in forest remote sensing (Kayitakire et al., 2006; Ouma & Tateishi, 2006), including two first order statistics (mean and variance). For instance, Wood et al. (2012) used mean, variance, entropy, and contrast for differentiating various vegetation structures, including grassland, savanna, and woodland. Kayitakire et al. (2006) found correlation and contrast were the most significant variables predicting forest features such as age, top height, stand density and basal area. Moreover, Homogeneity showed promising performance in forest segmentation based on forest stand age class (Franklin et al., 2010).

Table 3. 1: Description of GLCM texture features used in this study.

Texture Name	Description	Statistical formula	Reference
Contrast	Measures of the deviation between the intensities of neighboring pixels. Useful for capturing variability in the image.	$Cntr = \sum_{i,j=0}^{N-1} (i-j)^2 p(i,j)$	(Kayitakire et al., 2006)
Correlation	Correlation texture quantifies the linear dependence of gray levels on those of adjacent pixels. High correlation values indicate a linear relationship between neighboring pixel pairs' gray levels.	$Corr = \sum_{i,j=0}^{N-1} p(i,j) \frac{(i-\mu_i)(j-\mu_j)}{\sqrt{\sigma_i^2 \sigma_j^2}}$	(Kayitakire et al., 2006)
Dissimilarity	Instead of weighting the pixel values exponentially like contrast, dissimilarity increases linearly.	$Diss = \sum_{i,j=0}^{N-1} p(i,j) i-j $	(Kayitakire et al., 2014)
Angular-Second Moment	The angular second moment quantifies the uniformity or repetitions of pixel pairs. ASM has an inverse relationship with Entropy.	$ASM = \sum_{i,j=0}^{N-1} \{p(i,j)\}^2$	(Solberg, 1999)
Entropy	Measures the randomness of sparse matrix.	$Entr = - \sum_{i,j=0}^{N-1} p(i,j) \log[p(i,j)]$	(J. Zhou et al., 2017)
Homogeneity	Higher values indicate uniformity in the image pixels	$Homo = \sum_{i,j=0}^{N-1} \frac{p(i,j)}{1+(i-j)^2}$	(Park & Guldmann, 2020)

Where, the rows and columns of a spatial-dependence matrix (moving window) are denoted by i and j ; and the $p(i,j)$ represents the value of cell i,j in the matrix. N denotes the number of rows and columns. μ and σ are the weighted mean and variance of pixel values.

3.2. Calculation of GLCM Texture Features

Two first-order statistics and six second order GLCM texture features (table 3.1) were calculated separately from six spectral bands and one vegetation index. The selected spectral bands were Blue, Green, Red, Red-Edge, Nir-1, Panchromatic, and NDVI as vegetation indices. Coastal Blue and Nir-2 were not considered for texture calculation to save time since they produced similar results to the Blue and Nir-1 band, respectively, during forest metrics correlation analysis. The yellow band was also eliminated from further analysis because of its limited use in forest remote sensing.

Table 3. 2: GLCM parameter used for texture extraction.

Bands	Window Size	Displacement Length	Orientation
Multispectral	3*3 – 15*15 (6 Win. Sizes)	1 – 8 (6 Disp. Lengths)	0 - 135°and Avg. (5 Orientations)
Panchromatic	5*5 – 35*35 (6 Win. Sizes)	1 – 16 (7 Disp. Lengths)	0 - 135°and Avg. (5 Orientations)

The first-order statistics (Mean, Variance) were calculated based on the average and variance of all pixel values in a sampling plot. The second order GLCM texture features were calculated using the SNAP software considering three parameter values. These parameters were moving window size, displacement length, and orientation. Depending on the target object, the performance of texture features differs with different parameter selections. In this study, we considered GLCM parameters to capture differences from individual trees to Forest sampling plot level. The GLCM parameter selections are given in table 3.2. In this study we used a fifth orientation to calculate the textures which the value of the metric averaged over all orientations (Zhou et al., 2017), in addition to the four orientations employed in many of the studies (Bruniquel-Pinel & Gastellu-Etchegorry, 1998; Kayitakire et al., 2006; Ozdemir & Karnieli, 2011) to calculate GLCM textures. The sequence of steps taken from texture calculation to the prediction of forest metrics is given in fig. 3.1.

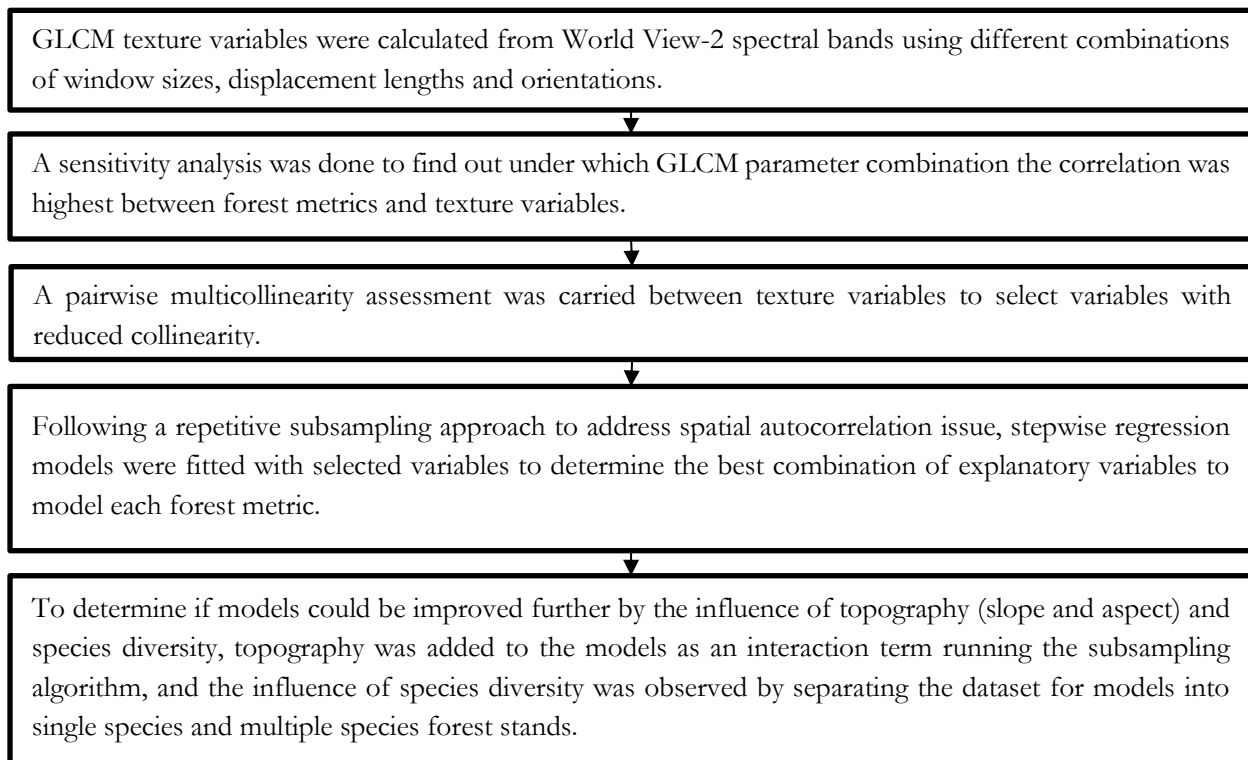


Figure 3. 1: Sequence of steps taken to achieve the research objectives.

3.3. Sensitivity Analysis of GLCM Parameter Selection

The influence of various GLCM parameter combinations was investigated to evaluate the sensitivity of textural features with varying window size, displacement length, and orientation to forest metrics. The second-order textures were calculated using different combinations of window size, displacement length, and orientation and these were tested against forest metrics. The performance was evaluated based on the correlation with forest metrics. Line charts were plotted to show how the correlation of textures with forest metrics changes with window sizes and displacement lengths following orientation degrees. The output of this sensitivity analysis is described in section 4.1. The parameter selection of highly correlated textures with forest metrics was used to select variables from thousands of texture features.

3.4. Selection of Predictor Variables and Colinearity Assessment

The texture variables selected for forest metrics using sensitivity analysis were analyzed for multicollinearity. The multicollinearity was assessed considering the correlation between the texture variables and the variance inflation factor (VIF) values. Texture variables with less than 70 percent correlation and VIF values of less than five were selected for prediction. In estimating the effect of collinearity, Dormann et al. (2013) mentioned correlation coefficient of 0.7 between variables and a VIF value of 10 as an indicator of collinearity, since exceeding this threshold begins to distort model estimation and subsequent prediction. The results of multicollinearity assessment for predictors of Mean DBH are represented and discussed in section 4.2.

3.5. Assessment of Spatial Autocorrelation

Spatial autocorrelation is a well-known problem for observational data in general and particularly for ecological spatial data (Rousset & Ferdy, 2014). In quantitative ecological studies, sampling design and size are critical since these research components affect the representativeness of data (Griffith, 2013) and influence the possibility of minimizing observational variances artificially (Mets et al., 2017). Sampling density can influence the spatial autocorrelation, which can cause the distortion of statistical distribution of the parameter (Cai & Wang, 2006). Therefore, it is essential to assess the magnitude and distance of spatial dependence in spatial ecological data. Geostatistical analyses of remotely sensed imagery typically use semi-variograms to model spatial autocorrelation to illustrate variances within a variable as a function of distance (Fleishman & mac Nally, 2006; M. Wulder & Boots, 1998).

In this study, the semi-variogram model was fitted to measure the range of spatial dependency in spectral bands using a total of 300 randomly distributed points. The semi-variogram plots are described in section 4.3. Based on the range of spatial autocorrelation (fig. 4.3), the field plots were subsampled as an approach to minimize the bias triggered by spatial autocorrelation. The process followed for subsampling and subsequent model fitting with subsampled datasets are described in section 3.6.

3.6. Subsampling of dataset and stepwise linear regression function

This study applied a subsampling function to create subsets of data from the entire dataset followed by a stepwise linear regression for 100 iterations. For subsampling, the study area was divided into grid cells with a certain distance based on the range of spatial autocorrelation. Then, the subsampling function generates a data subset by randomly picking a single sampling plot from every grid cell in each iteration (fig. 3.4). This subsampling method assures that plots are selected at a certain distance and minimal effect of spatial autocorrelation in the variables.

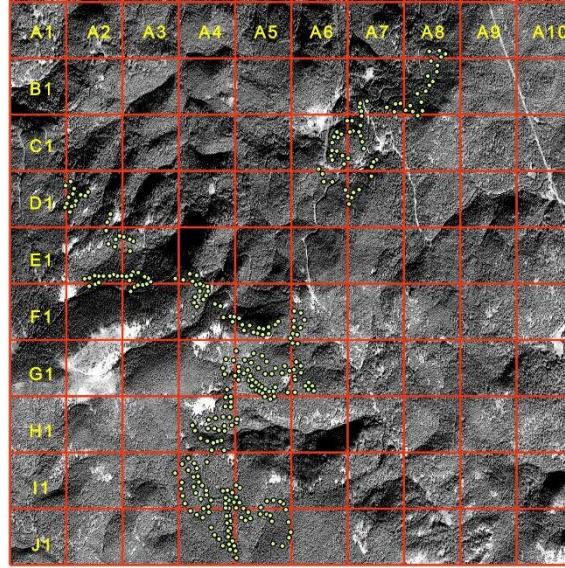


Figure 3. 2: sampling plots assigned to 500m grids.

The data subsets created in each iteration were then fitted with stepwise linear regression. For each iteration, stepwise regression selected the texture variables that explain most of the variability in the forest metrics. From the stepwise models fitted between forest metrics and the texture variables, the significance of predictor variables was estimated at confidence interval of 95% and 99%. After 100 iterations, the number of times that each textural variable was included in the model and the number of times that it was significant at the 95% and 99% confidence intervals were then plotted as a bar chart. The best two texture variables were then selected based on the number of times those variables became significant. Best two predictors were used to fit the base model using bootstrap stepwise regression to predict the forest metrics. The base model can be shown in the following way:

$$\text{Model}_{\text{Base}}: RV = \beta_0 + \beta_1 X_1 + \beta_2 X_2 \quad (6)$$

Where,

RV = response variable,
 X_1 and X_2 are two predictor texture variables.

$\text{Model}_{\text{Base}}$ outputs also includes the prediction of forest metrics as well as the regression coefficients and significance values of variables, and summary statistics such as R^2 and RMSE Values.

3.7. Assessment of topographic variables influence on forest metrics prediction

To incorporate the topographic influence into $\text{Model}_{\text{Base}}$, we used degree of Slope and standardized slope aspect (ASP) in the bootstrap stepwise regression model as an interaction term. The models developed using slope ($\text{Model}_{\text{Slope}}$), ASP ($\text{Model}_{\text{ASP}}$) and combined influence of slope and ASP ($\text{Model}_{\text{Com}}$) are described using Equations 6, 7 and 8.

$$\text{Model}_{\text{Slope}}: RV = \beta_0 + \beta_1 X_1 + \beta_2 X_2 + \beta_3 X_1 \times \text{slope} + \beta_4 X_2 \times \text{slope} \quad (7)$$

$$\text{Model}_{\text{ASP}}: RV = \beta_0 + \beta_1 X_1 + \beta_2 X_2 + \beta_3 X_1 \times \text{ASP} + \beta_4 X_2 \times \text{ASP} \quad (8)$$

$$\text{Model}_{\text{Com}}: RV = \beta_0 + \beta_1 X_1 + \beta_2 X_2 + \beta_3 X_1 \times \text{slope} + \beta_4 X_2 \times \text{slope} + \beta_5 X_1 \times \text{ASP} + \beta_6 X_2 \times \text{ASP} \quad (9)$$

Where,

RV = Response variables,

$\beta_0, \beta_1, \dots, \beta_6$ = Regression parameters to be computed from the model and X_1, X_2 are the texture variables as predictor.

The models of topographic variable interaction (Eq. 6,7, and 8) were then compared with Model_{Base} using the corrected Akaike information criterion (AICc) values. AICc is a mathematical approach for measuring how well a model fits the data it was derived from, when the sample size is small, and a lower AICc value implies a better fit of the model (Brewer et al., 2016). Models' performances were also explained using R^2 and RMSE values.

3.8. Assessment of Species Diversity Impact of Forest Metrics Prediction

The best model fitted for each forest metric was then compared in terms of forest stand species diversity. The sampling plots were grouped into single species and multiple species plot classes to compare the impact of species diversity in the model prediction. The grouping was based on SDI values (table 2.1), where a 0 value indicates plots of single-species forest stands, and an SDI value greater than 0 indicates forest stands with multiple species. The SDI thresholding grouped 296 sampling plots into 59 multiple species plots and 237 single species plots. For a fair comparison of models, the single species models for forest metrics prediction were fitted using 59 randomly chosen plots. A two-tailed t-test was conducted to test the statistical significance of the difference between the forest metrics prediction obtained from single and multiple species plots. The model's performance was also evaluated by average R^2 and RMSE values.

4. RESULTS

The following sections describe the results of the variable selection process (sensitivity and multicollinearity analysis) and data distribution handling. Then, it presents the relationship between forest metrics and remote sensing variables and the influence that topography has on this relationship. Moreover, this section compares the prediction accuracies of forest metrics from different topographic effect models, as well as the prediction accuracy of forest metrics models fitted using data from different species diversity forest plots.

4.1. Determining the best combination of GLCM paramters

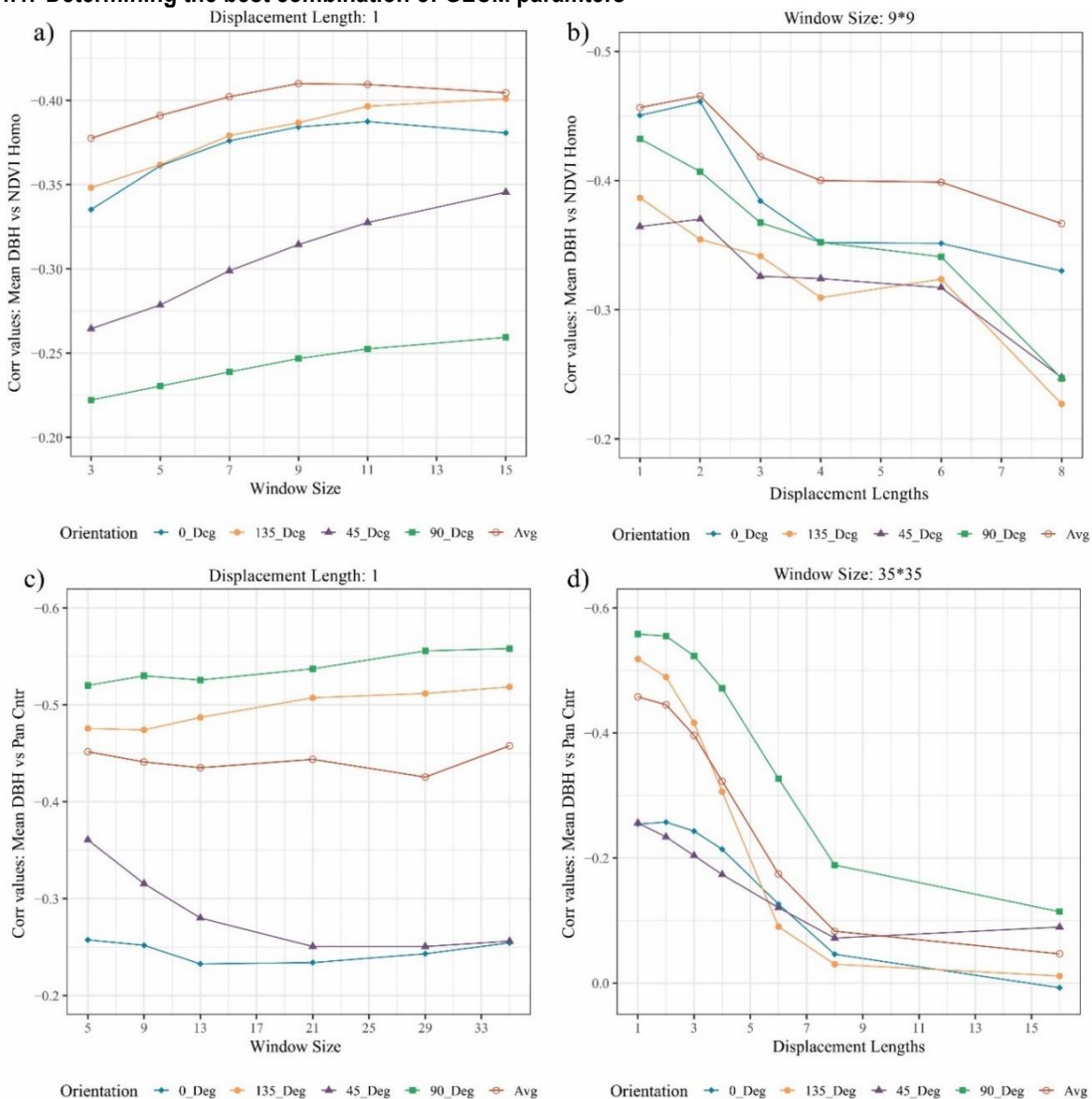


Figure 4. 1: Correlation of texture features with different parameter settings and Mean DBH. a) NDVI Homogeneity with varying window sizes and orientations, b) NDVI Homogeneity with varying displacement length and orientations, c) Pan Cntr with varying window sizes and orientations, and d) Pan Cntr with varying displacement length and orientations.

The sensitivity analysis of texture features resulted in different correlation coefficient values between forest metrics and texture features as the GLCM parameters changed. An example of how GCLM parameters

influence the correlation between texture variables and forest stand metrics is depicted in Fig. 4.1. Fig. 4.1a and c show how the correlation between homogeneity texture from NDVI and contrast from panchromatic with Mean DBH changes with window sizes and orientation with a fixed displacement length of 1. Textures calculated from multispectral bands such as NDVI homogeneity with an average orientation showed consistently higher correlation coefficients with Mean DBH, where 90° was the most consistent orientation degree for panchromatic contrast. In addition, an increasing correlation was observed as the window size increased (fig. 4.1a and c). Nevertheless, the increase in correlation value plateaued around 9*9 window size for NDVI homogeneity and 35*35 window size for panchromatic contrast. After 2 pixels of displacement, the correlation coefficient for both textures tended to decline as the length increased (fig. 4.1 b and d); however, contrast from the panchromatic band showed highest correlation with Mean DBH at displacement length of 1. Therefore, we chose the NDVI homogeneity texture feature calculated with window size 9*9, displacement length 2, and the average of orientations, and the panchromatic contrast texture feature calculated with window size 35, displacement length 1, and the 90-degree orientations, out of hundreds of other possible combinations of GLCM parameters, to determine the Mean DBH.

It is important to report that selected window sizes (9*9 and 35*35) roughly represent the dimension of the field plots, which were 15.8 m in diameter. Also, given the study area's tree canopy diameters range from 3 to 8 m, the selected displacement for panchromatic texture indicates that panchromatic textures are sensitive to each pixel variation within the canopy, whereas multispectral texture's displacement length of 2 pixels (3.2 m at ground) indicate the sensitiveness at a comparatively larger distance that might be able to capture differences at canopy edge.

Similar sensitivity analysis was carried out for other textures variables with Mean DBH and also with Tree Count and SD DBH. Tree count yielded identical results to Mean DBH, however SD DBH yielded different outcome in terms of displacement length of multispectral textures, an example of which is shown in annex 1. Multispectral textures such as contrast from green band showed highest correlation with SD DBH at a displacement length of 5. Which indicate texture variables best correlate with SD DBH when the variabilities are captured at a larger distance.

4.2. Collinearity among texture variables

The multicollinearity assessment of texture variables selected in the previous step showed a very high correlation between them when they were taken from the same spectral band. Therefore, we selected a single texture feature from each of the bands. Fig. 4.2 exhibits the correlation between texture variables selected for Mean DBH and their VIF values. The correlation coefficient between the variables below 70 percent and the VIF values below 5 confirmed a negligible collinearity issue in the predictor variables. The correlation plots of variables for Tree Count and SD DBH are given in Annex 2.

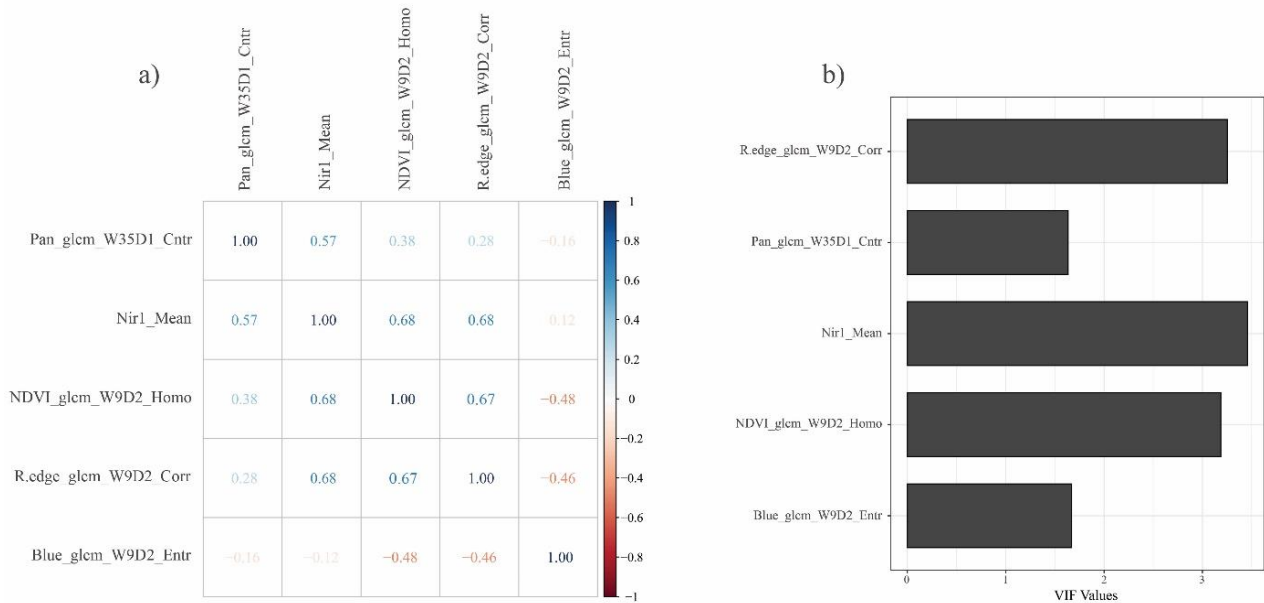


Figure 4. 2: Plots showing a) correlation among texture variables and b) VIF values.

4.3. Spatial dependency of data

Semi-variogram models were fitted for values of each spectral band to assess the range of spatial autocorrelation within the data. Fig. 4.3 shows the range of spatial autocorrelation in Nir-1, NDVI and Panchromatic bands. The range of spatial autocorrelation for multispectral bands was found around 500m where the range for panchromatic band is about 200m. The average distance ($\pm 45m$) between field plots falls shorter than the range of spatial dependence in remote sensing images, implying spatial dependency in predictor variables.

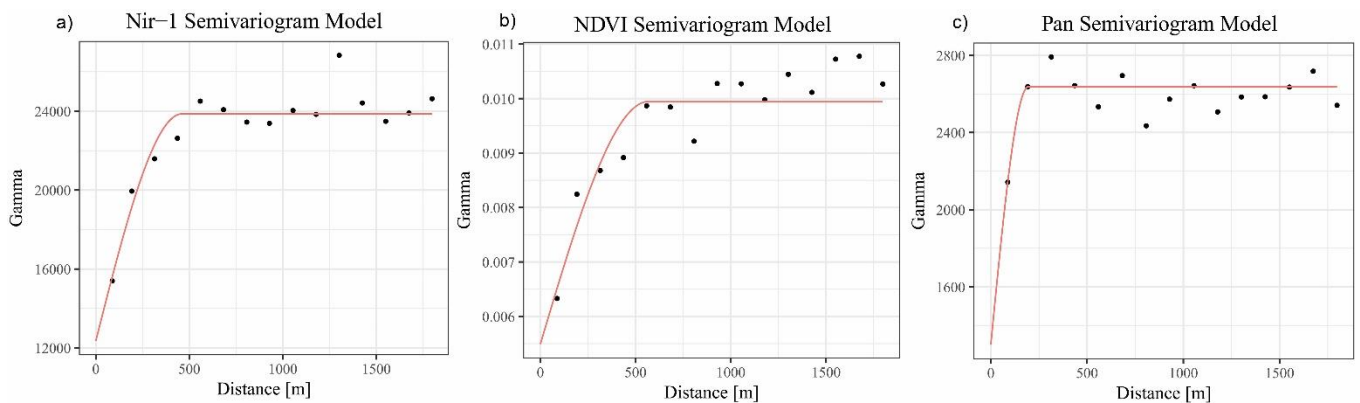


Figure 4. 3: Semi variogram model showing the range of spatial dependence around neighbouring pixels of a) Nir-1 b) NDVI c) Panchromatic bands.

4.4. Correlation and Significance of Texture Variables with Forest Metrics

The pairwise Pearson correlation assessment between the forest metrics and texture variables demonstrated that the individual forest metric presents differentiating results (table 4.1). The second-order textures (contrast and correlation) calculated from the panchromatic band showed the highest correlation with each of the forest metrics compared to texture variables from multispectral bands. Correlation texture computed from the panchromatic band had the strongest positive correlation with SD DBH ($r = 0.41$), but negatively correlated with Tree Count ($r = -0.56$) and contrast from panchromatic band was the highest correlated variable with Mean DBH ($r = -0.57$). Mean of grey levels calculated from Nir-1 band was the only first order statistical variable found significantly correlated with Mean DBH ($r = -0.49$). Moreover, entropy from the

blue band was least correlated variable with Mean DBH ($r = 0.33$), however strongly correlated with Tree count ($r = -0.51$). Contrast texture from Nir-1 band found to be the least correlated variable for SD DBH.

Table 4. 1: Pearson correlation coefficients between forest metrics (Mean DBH, SD DBH, Tree Count) and selected texture variables. (W = window size, D = displacement length and O = orientation)

	Texture Variables	W	D	O	Pearson Correlation (r)	P-value
Mean DBH	Pan Cntr	35	1	90°	-0.57	$p < 0.01$
	Nir-1 Mean	-	-	-	-0.49	$p < 0.01$
	NDVI Homo	9	2	Avg.	-0.47	$p < 0.01$
	R.edge Corr	9	2	Avg.	-0.40	$p < 0.01$
	Blue Entr	9	2	Avg.	0.33	$p < 0.01$
SD DBH	Pan Corr	35	1	90°	0.41	$p < 0.01$
	Blue Diss	9	5	Avg	0.39	$p < 0.01$
	Green Cntr	9	5	Avg	0.36	$p < 0.01$
	R.edge Diss	9	5	Avg	0.34	$p < 0.01$
	Nir-1 Cntr	9	4	Avg	0.29	$p < 0.01$
Tree Count	Pan Corr	35	1	90°	-0.56	$p < 0.01$
	Blue Entr	9	2	Avg	-0.51	$p < 0.01$
	R. edge Corr	9	3	Avg	0.50	$p < 0.01$
	Green Diss	9	2	Avg	-0.48	$p < 0.01$
	NDVI Entr	9	2	Avg	0.47	$p < 0.01$

Fig. 4.4 exhibits the number of times texture variables were included as significant variables after a stepwise regression carried out on subsamples of dataset as described in section 3.6. Panchromatic contrast was found the most frequently (66 times out of 100 at $p < 0.05$) selected explanatory variable to explain Mean DBH and panchromatic correlation was found the most important variable for explaining SD DBH and Tree Count becoming significant for 37 and 56 times, respectively, at $p < 0.05$.

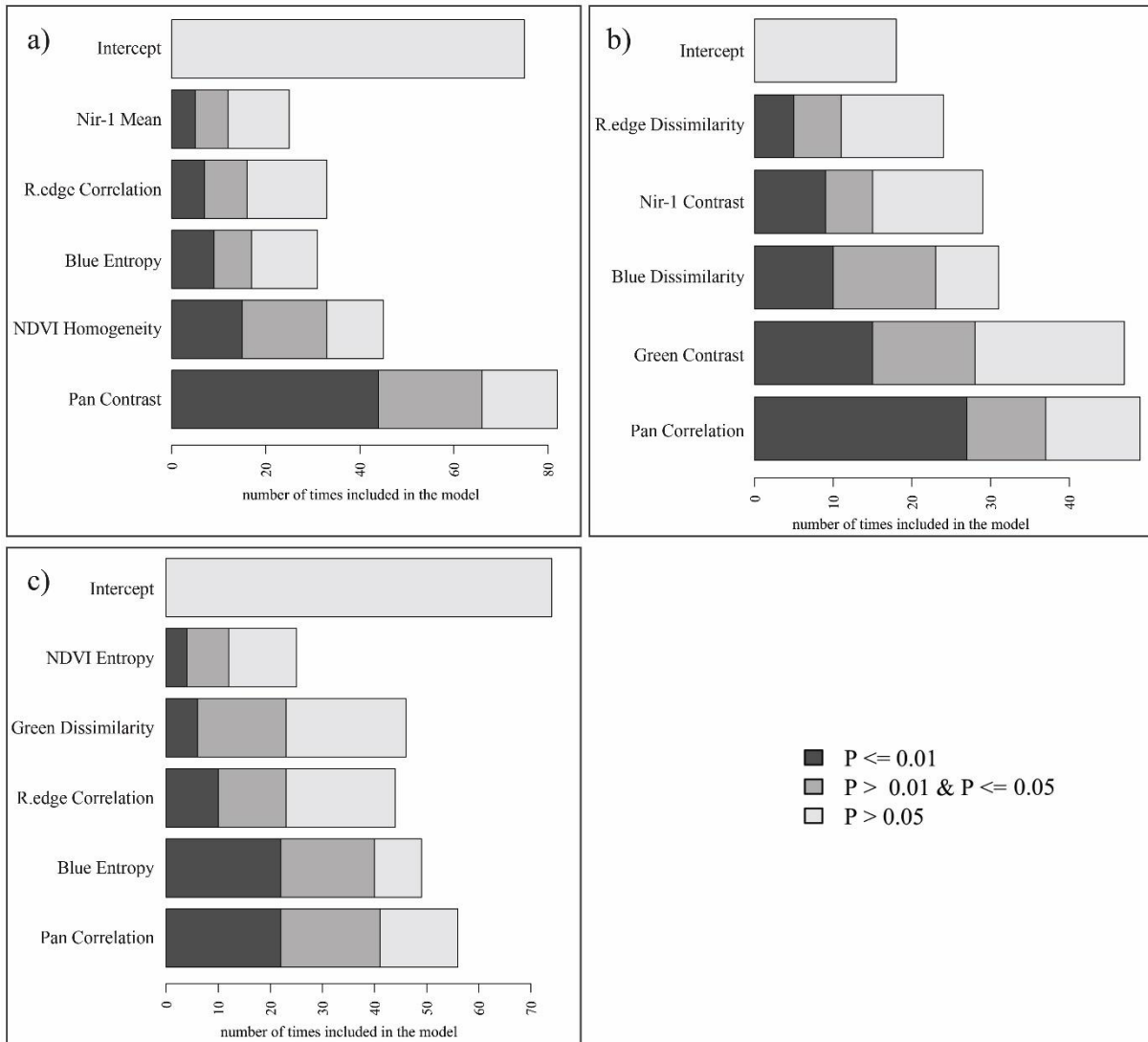


Figure 4. 4: Variable significance plot showing the texture variables selected for forest metrics a) Mean DBH, b) SD DBH, c) Tree Count; and the number of times they became significant at $\alpha = 0.01$ and 0.05 .

At $p < 0.05$, homogeneity from NDVI band, contrast from green band, and entropy of blue band were statistically significant for Mean DBH, SD DBH, and Tree Count about 32, 28, and 39 times, respectively. Two variables being significant most frequently for each of the forest metric were selected to develop the prediction model (Model_{Base}), given in table 4.2. Subsequently, these variables were used to explore how topography and species diversity affect their performance in prediction model.

Table 4. 2: Texture variables selected for developing Model_{Base}.

Mean DBH	SD DBH	Tree Count
Panchromatic contrast	Panchromatic correlation	Panchromatic correlation
NDVI homogeneity	Green contrast	Blue entropy

4.5. Topographic Influence on Variable Relationship with Forest Metrics

In predicting forest metrics, the interaction effects of slope, aspect, and their combined influence on texture variables are given in table 4.3 and fig. 4.5 represents the frequency of variable significance for Mean DBH.

As seen in the table, Mean DBH had a negative relation with contrast from panchromatic band (-7.76) and homogeneity from NDVI (-184.73) in Model_{Base}. In interaction with slope in Model_{Slope}, the negative coefficients of both variables (-0.18 and -7.09) suggest an even stronger relationship with Mean DBH, and the relationship becomes more negative as slope increases. The variable significance plot (fig. 4.5a) for Model_{Slope} shows that, panchromatic contrast and NDVI homogeneity with slope interaction effect were selected more frequently as significant variable (56 and 42 times, respectively, at $p < 0.05$) for Mean DBH than just the main effect of panchromatic contrast and NDVI homogeneity. In Mean DBH Model_{ASP}, aspect interacted panchromatic contrast texture showed an increased relationship with Mean DBH and the interaction effect between panchromatic contrast and aspect was most often significant than just the main effect of panchromatic contrast (fig. 4.5b). On the other hand, the relation between Mean DBH and homogeneity of NDVI reduced at sites that had higher values for their aspect. Moreover, in the model that combined interactions of both slope and aspect, the most significant variables found were the interaction terms of slope followed by the texture variables as main effects, and not the interactions of aspect.

Table 4. 3: Coefficients of regression and p-values for variables from four different models of Mean DBH, SD DBH, and Tree Count. Values indicate average of 100 iterations of the models following the subsampling of dataset.

	Variables	Model _{Base}		Model _{Slope}		Model _{ASP}		Model _{Com}	
		Reg. Coeff	p-val	Reg. Coeff	p-val	Reg. Coeff	p-val	Reg. Coeff	p-val
Mean DBH	Panchromatic Contrast	-7.76	0.03	-8.42	0.02	-8.34	0.02	-9.75	0.03
	NDVI Homogeneity	-184.7	0.05	-144.2	0.04	-254.1	0.04	-129.5	0.05
	Slope	-	-	1.51	0.03	-	-	1.46	0.02
	Panchromatic Contrast: Slope	-	-	-0.18	0.01	-	-	-0.12	0.02
	NDVI Homogeneity: Slope	-	-	-7.09	0.03	-	-	-9.84	0.04
	Aspect	-	-	-	-	31.34	0.04	11.70	0.06
	Panchromatic Contrast: Aspect	-	-	-	-	-10.05	0.05	-6.83	0.07
	NDVI Homogeneity: Aspect	-	-	-	-	96.63	0.04	174.50	0.08
SD DBH	Panchromatic Correlation	181.82	0.02	185.48	0.05	191.96	0.03	233.56	0.05
	Green Contrast	0.13	0.03	-0.11	0.05	-0.01	0.05	-0.19	0.06
	Slope	-	-	-0.68	0.05	-	-	-1.186	0.05
	Panchromatic Correlation: Slope	-	-	0.25	0.05	-	-	0.71	0.05
	Green Contrast: Slope	-	-	0.01	0.06	-	-	0.01	0.05
	Aspect	-	-	-	-	-185.4	0.05	-70.27	0.05
	Panchromatic Correlation: Aspect	-	-	-	-	161.53	0.04	50.05	0.04
Green Contrast: Aspect	-	-	-	-	0.20	0.05	0.34	0.04	
Tree Count	Panchromatic Correlation	-151.5	0.02	-240.1	0.03	-147.3	0.03	-299.7	0.04
	Blue Entropy	-10.43	0.02	-15.69	0.04	-8.59	0.02	-5.52	0.05
	Slope	-	-	-4.18	0.05	-	-	-6.51	0.06
	Panchromatic Correlation: Slope	-	-	3.24	0.04	-	-	4.60	0.06
	Blue Entropy: Slope	-	-	0.19	0.05	-	-	0.22	0.06
	Aspect	-	-	-	-	75.34	0.03	41.30	0.06
	Panchromatic Correlation: Aspect	-	-	-	-	61.96	0.03	122.65	0.06
	Blue Entropy: ASP	-	-	-	-	-21.01	0.04	-27.08	0.07

In SD DBH Model_{Slope}, the regression coefficients of slope interacted panchromatic correlation (0.25) and green contrast (0.01) indicate that at steep slopes the relation between SD DBH and panchromatic correlation become stronger while a reduced relationship was observed with green contrast. Accordingly, panchromatic correlation with slope interaction effect became the most frequently significant variable (36

times at $p < 0.05$) for SD DBH and slope interacted green contrast was the least frequent significant variable (Annex 3a). Similar result was obtained with the interaction effect of aspect on texture variables in SD DBH Model_{ASP}. However, in the combined model, aspect interacted texture variables were most frequently added in the model as significant variable. Variables with slope interaction term showed very little difference with the main texture variables in terms becoming significant to explain SD DBH.

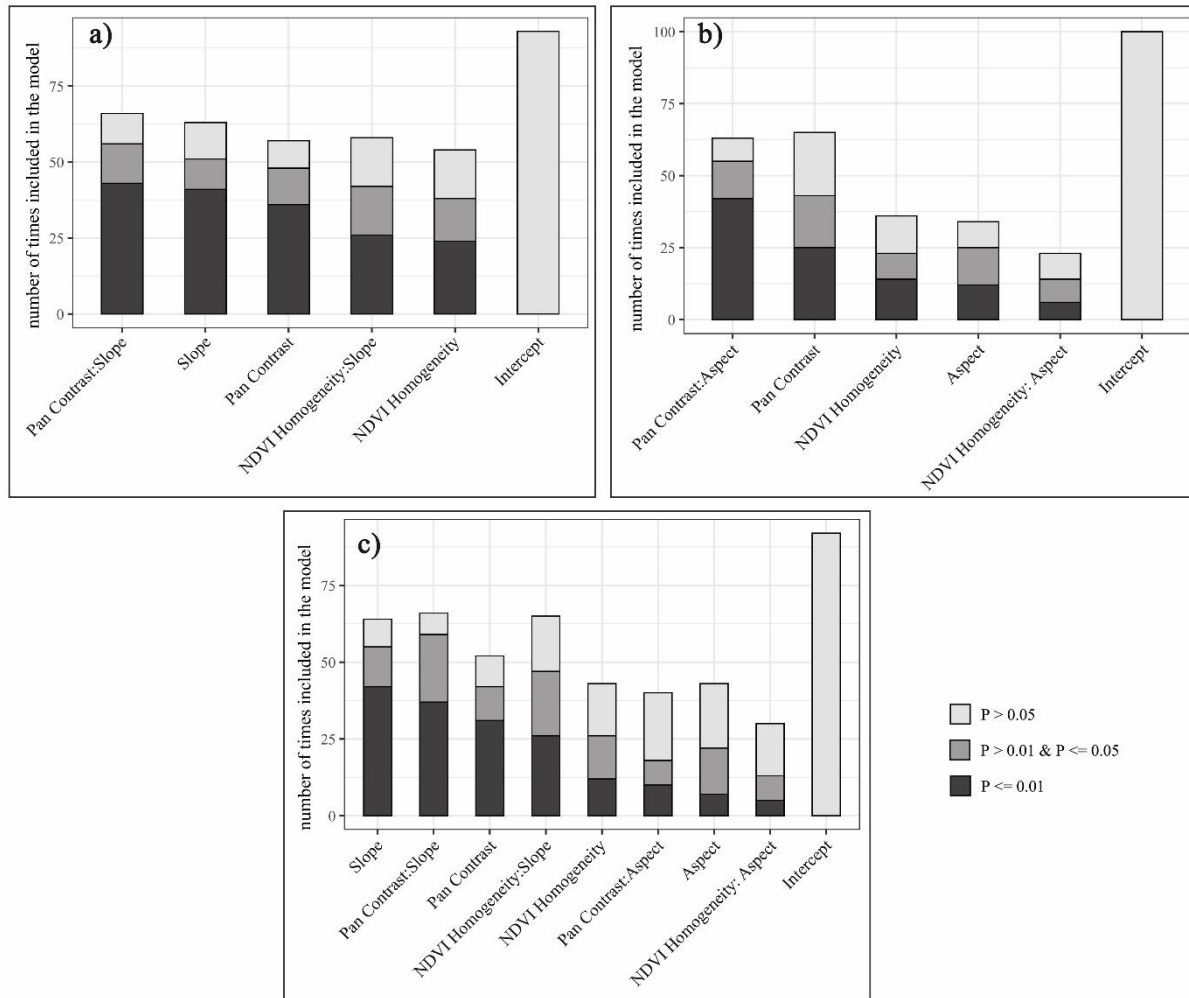


Figure 4. 5: Variable significance plot for Mean DBH a) Model_{Slope} b) Model_{ASP} c) Model_{Com}, showing the number of times the variables were included in the model and became significant at $\alpha = 0.01$ and 0.05 .

The panchromatic correlation and blue entropy variables with interaction effect of aspect demonstrated a poor relationship with Tree Count, indicating that on steep slopes, the relationship between texture variables and tree count weakens. Therefore, the interaction of panchromatic correlation and blue entropy with aspect was less often significant than just the main effect of these texture variables (Annex 4a).

4.6. Performance of models for forest metrics prediction

Three statistical indicators (R^2 , RMSE, and AICc) were used to assess the goodness of fit of models developed for forest metrics. The R^2 , RMSE and AICc values of four models for each forest metric derived from 100 iterations are presented in figures 4.6. As can be seen from the figures, ModelBase was the least performing model for all three forest metrics, achieving average R^2 values of 0.40, 0.30, and 0.31, and average RMSE values of 7.06, 4.62, and 3.91 respectively for Mean DBH, SD DBH, and Tree Count.

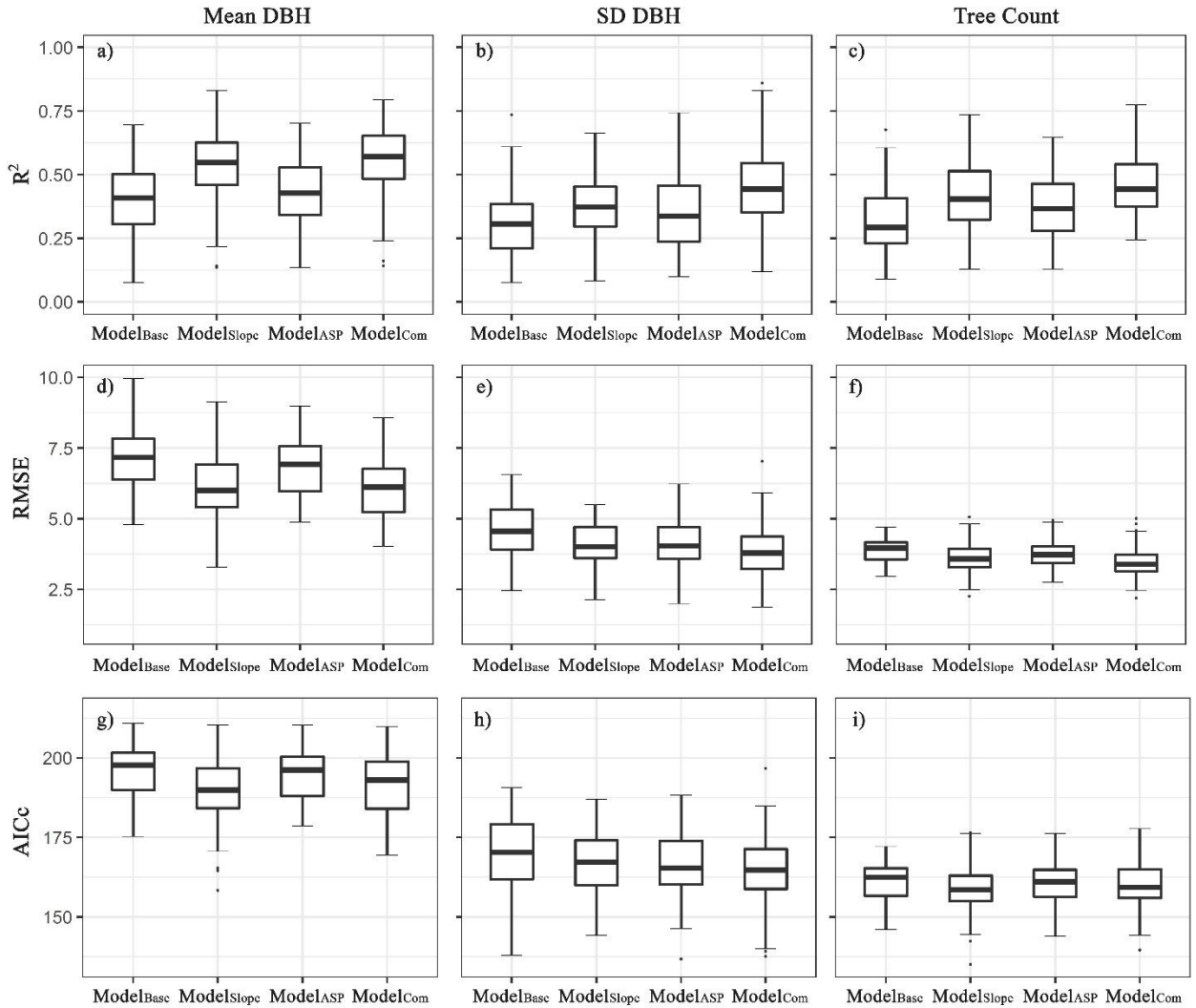


Figure 4. 6: Boxplots showing the R^2 , RMSE and AICc distribution for Mean DBH (a,d,g); the R^2 , RMSE and AICc distribution for SD DBH (b,e,h); and the R^2 , RMSE and AICc distribution for Tree Count (c,f,i).

For Mean DBH, the combined model having the interaction effect of both slope and aspect ($Model_{Com}$) yielded the highest average R^2 of 0.56, followed by $Model_{Slope}$ (0.54) and $Model_{ASP}$ (0.43). However, $Model_{Slope}$ of Mean DBH presented a better fit of the data with lowest average RMSE (6.03) and AICc value (189.19). For SD DBH, $Model_{Com}$ outperformed other models in terms of R^2 , RMSE, and model fitness ($AICc = 164.76$). Similarly, $Model_{Com}$ produced the highest average R^2 and lowest average RMSE values for Tree Count; however, Tree Count $Model_{Slope}$ fitted the data slightly better than $Model_{Com}$.

From the assessment, it was evident that 1) there were minimal differences in the interquartile range of the statistical indicators (R^2 , RMSE, and AICc) among all four models for each forest metric; 2) incorporating topographic influences on $Model_{Base}$ fit the data better because the $Model_{Slope}$, $Model_{ASP}$, and $Model_{Com}$ had lower AICc values than $Model_{Base}$; 3) $Model_{Com}$ for each forest metric showed comparatively higher R^2 and lower RMSE than other models, but this model can overfit the data in most cases; and the Slope-influenced models performed better than ASP model in terms of R^2 , RMSE, and AICc values.

Fig. 4.7 compares field measured values, and their estimates predicted from the best-fitted models for Mean DBH, SD DBH and Tree Count. The scatter plot of Mean DBH (fig. 4.7a) shows a non-linear fit of the predicted values with observed values. As can be seen, the predicted values tend to saturate at Mean DBH values greater than 30 cm. The scatterplots of SD DBH (figure 4.7b) and Tree Count (figure 4.7c) illustrate

that prediction models for these two metrics overestimated SD DBH and Tree Count at lower values and underestimated them at higher values.

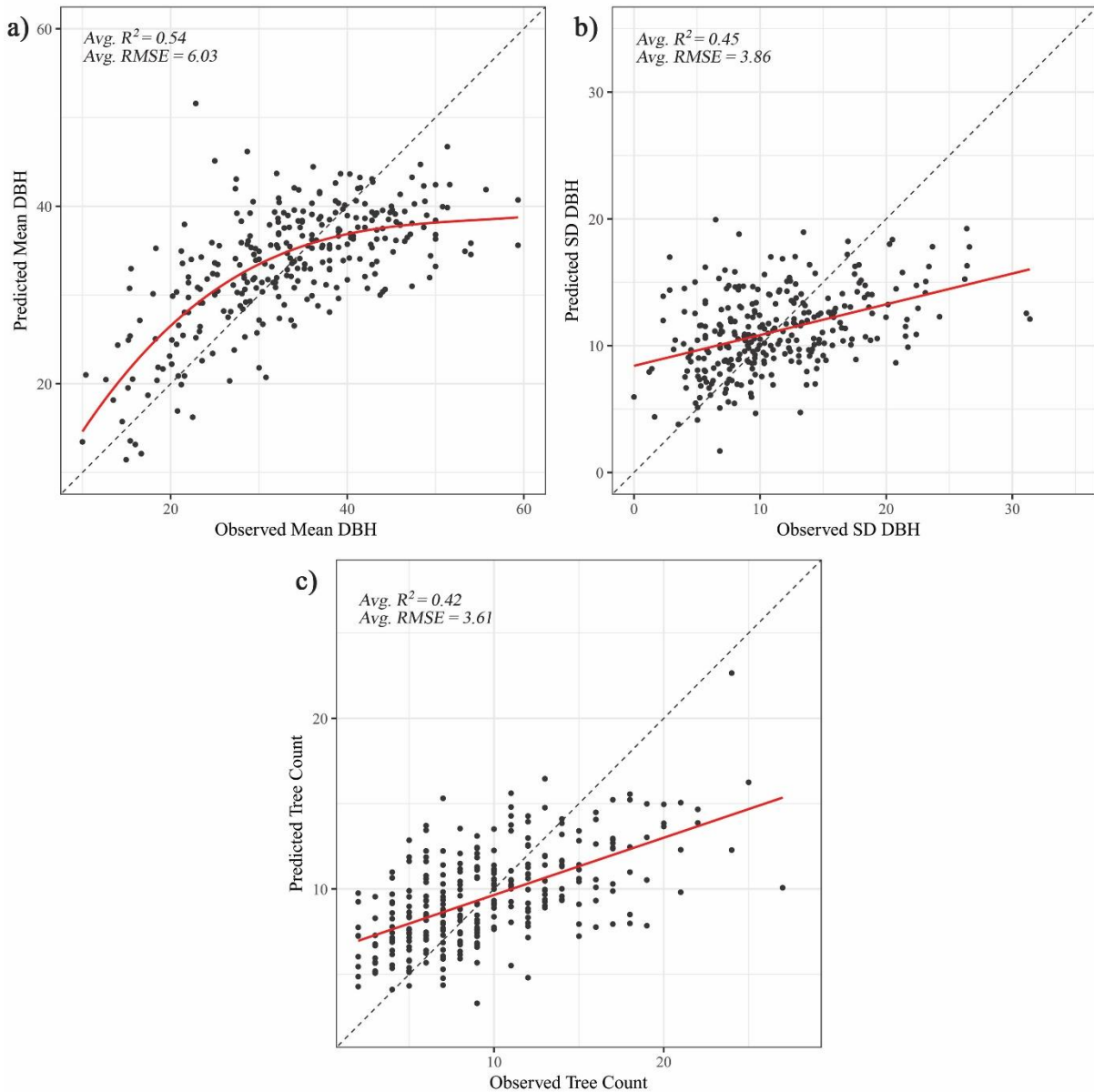


Figure 4. 7: Field measured forest metrics vs. predicted forest metrics values from best fitted models a) Mean DBH Model_{Slope}, b) SD DBH Model_{Com}, c) Tree Count Model_{Slope}. Predicted values are the average from 100 different models.

4.7. Species diversity influence on forest metrics prediction

When comparing plots that consist of a single tree species against plots that hosted multiple tree species, the data distribution of Mean DBH, SD DBH, and Tree Count show that single species plots have larger average values for Mean DBH whereas lower average values for Tree Count and SD DBH (Fig. 4.8a, d, g). The contrast and correlation textures from panchromatic band exhibited a similar pattern as the forest metrics in different species diversity plots. In contrast, the texture variables from multispectral bands such as homogeneity from NDVI and entropy from blue band showed an opposite pattern to Mean DBH and Tree Count, respectively. However, the interquartile ranges of forest metrics and image textures imply smaller variability in single-species plots' data distribution compared to multiple species plots (fig. 4.8).

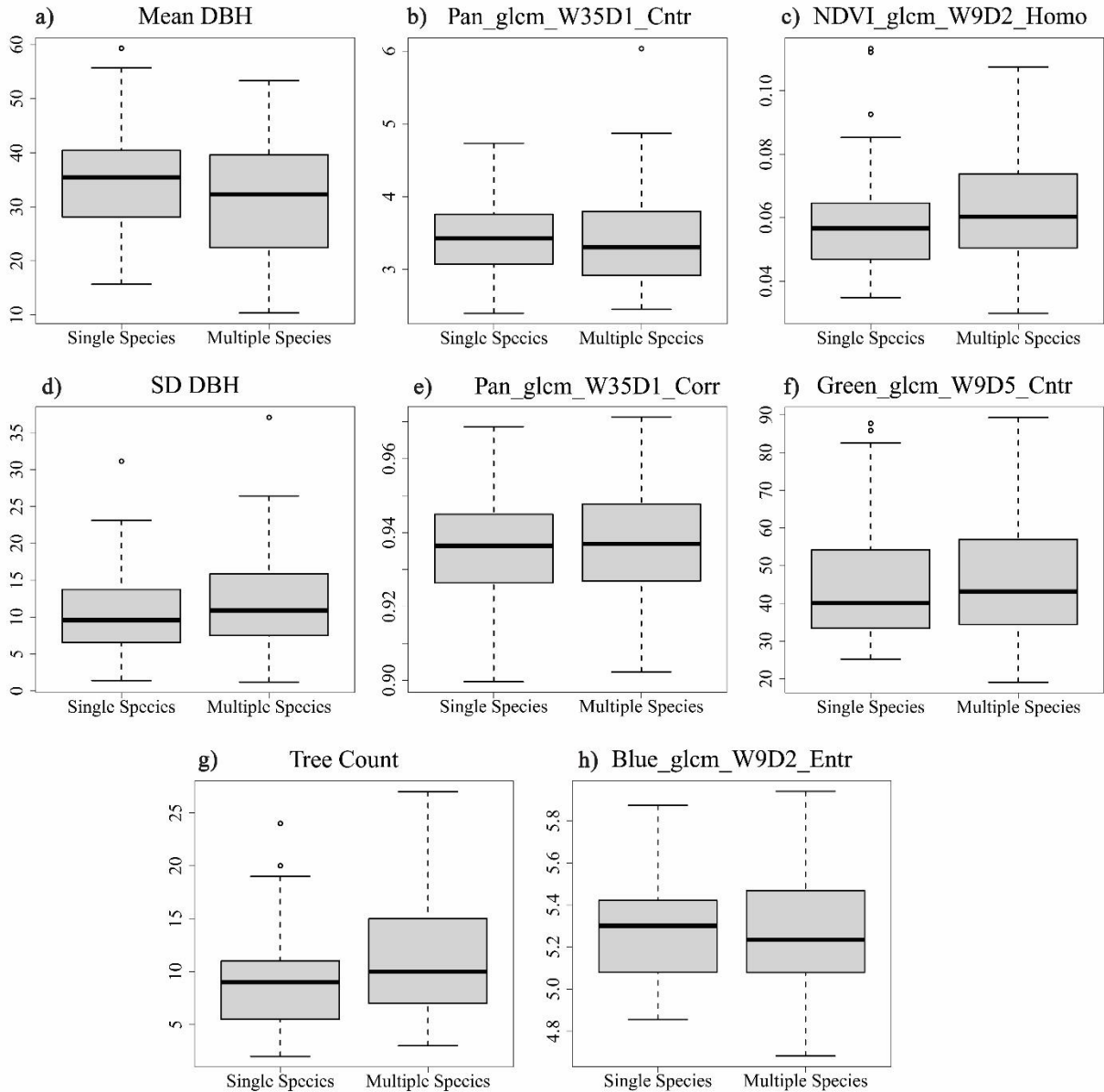


Figure 4. 8: Boxplot summaries of the forest metrics and image texture characteristics in single species and multiple species forest plots.

The model fitting for Mean DBH, SD DBH, and Tree Count is compared in fig. 4.9 for single species and multiple species plots, and table 4.4 shows the regression model statistics as well as the t values comparing the models R^2 and RMSE for single species plots and multiple species plots. The fitting of regression models shows that Mean DBH and Tree Count were better predicted in single-species plots. Models trained on data from single-species plots were 11% and 8% more accurate at predicting Mean DBH and Tree Count, respectively, than those trained on data from multiple species (table 4.4). Also, the Average RMSE values of Mean DBH and Tree Count values were smaller for single species plot models. However, SD DBH is better predicted in multiple species plots achieving an average R^2 value of 0.68 and average RMSE of 2.80 (table 4.4).

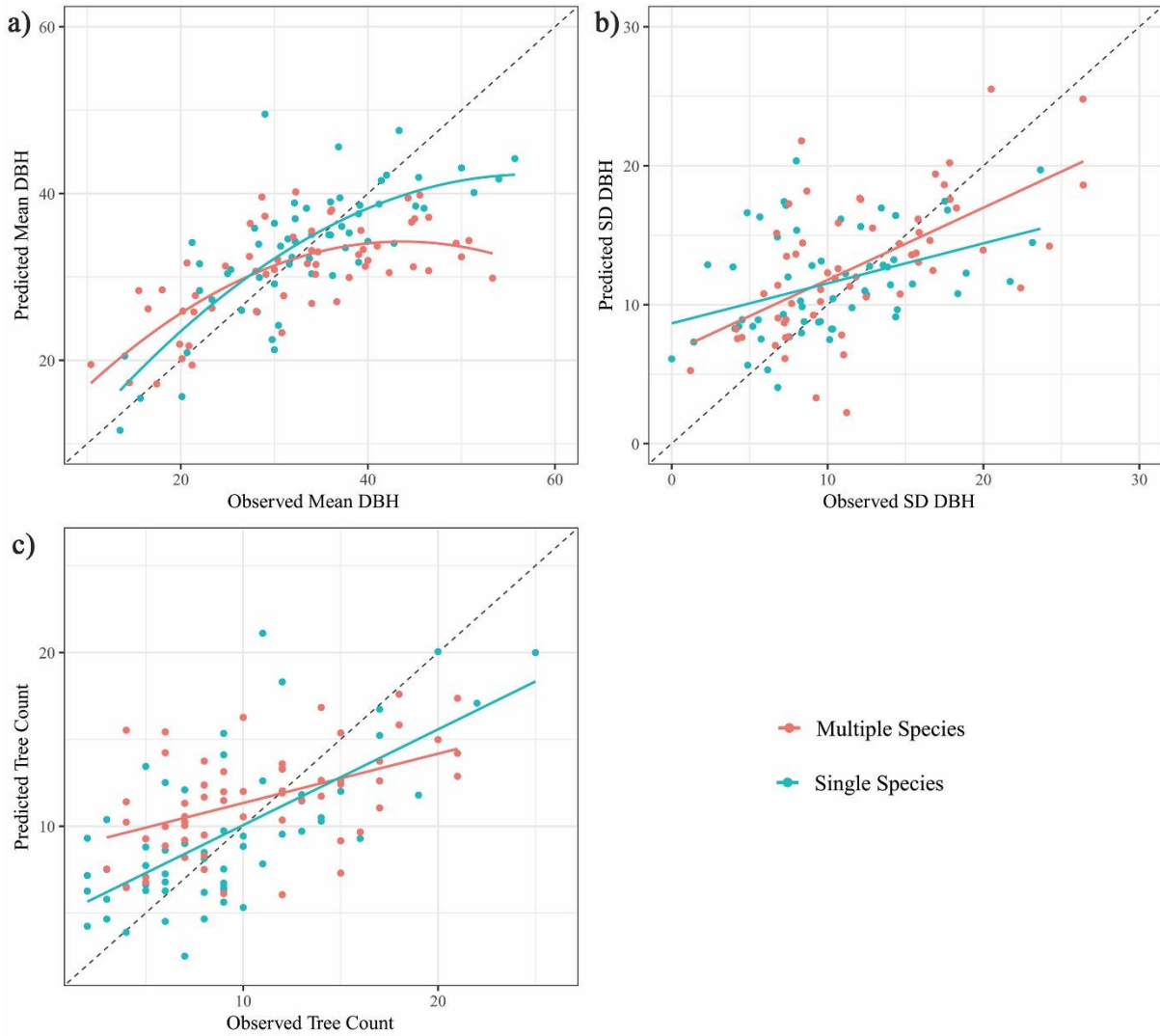


Figure 4. 9: Scatterplots of predicted vs. observed a) Mean DBH, b) SD DBH, c) Tree count in single species and multiple species plots.

Using a two sampled t-test, the prediction accuracies (R^2 and RMSE) of each forest metric model, fitted for single species forest plots were compared to those in multiple species forest plots. For each forest metric, the R^2 and RMSE were significantly different for models fitted with data from single species forest plots versus models fitted with data from multiple species forest plots, as shown by t values in table 4.4. The t-values comparing the R^2 for Mean DBH, SD DBH and Tree Count are 5.51, -9.29, and 4.13, respectively.

The negative t-value for SD DBH indicates that the SD DBH model fitted for multiple species forest plots produced a higher mean of R^2 than the model fitted for single species plots. On the other hand, the positive t-value for SD DBH when comparing the RMSE, it indicates that the SD DBH model fitted for multiple species forest plots produced a lower mean of RMSE than the model fitted for single species plots.

Table 4. 4: Average and standard deviation of R² and RMSE values of Mean DBH, SD DBH, and Tree Count in single species and multiple species plots (n = 59). The t statistics indicate the differences in the obtained R² and RMSE from models fitted with data from single species plots and multiple species plots.

	Mean DBH				SD DBH				Tree Count			
	Avg. R ²	Avg. RMSE	t-val R ²	t-val RMSE	Avg. R ²	Avg. RMS E	t-val R ²	t-val RMSE	Avg. R ²	Avg. RMS E	t-val R ²	t-value
Single Species	0.6 (± 0.15)	5.7 (± 0.82)	5.51 (p<.01)	-7.84 (p<.01)	0.49 (± 0.12)	3.72 (± 0.73)	-9.29 (p<.01)	8.01 (p<.01)	0.5 (± 0.14)	3.48 (± 0.44)	4.13 (p=.01)	-2.38 (p<.01)
Multiple Species	0.49 (± 0.13)	7.06 (± 1.51)			0.68 (± 0.17)	2.8 (± 0.88)			0.42 (± 0.13)	3.91 (± 0.54)		

5. DISCUSSION

5.1. The importance of GLCM texture feature and their parameter selection in determining the relationship with Forest metrics

One of the important objectives of this study was to assess the relationship of remote sensing based texture variables with forest metrics. An apparent influence on the relationship was observed from the spatial resolution of textures and selection of textures and the parameter selection used to calculate the textures. In this study, the obtained relationship between forest metrics and texture variables was much stronger for texture features calculated from a panchromatic band with a resolution of 0.4m than for textures from a multispectral band with a resolution of 1.6m. One probable explanation is that the fine-grained textures from the panchromatic band captured the canopy surface roughness more accurately. In a Norway spruce forest, Stellingwerf & Hussin (1997) compared the predicted number of stems from different scale infrared photos to the number of trees measured on the field. When images at a 1:5000 scale were utilized, the correlation coefficient between them was 0.92, but it reduced to 0.72 when 1:10000 scale images were used.

In determining the strength of forest metrics and texture relationship, we observed that the correlation is sensitive to the selection of all three GLCM parameters such as window size, displacement length, and orientation degree. Wang et al. (2015) argued that selecting the best-performed parameter is not straightforward and mainly depends on the canopy characteristics of the forest stand. There are several methods for identifying the parameters used to calculate textures. For instance, Franklin et al. (1996) employed a number of experimental semi-variograms to determine the optimum texture window size for use in remote sensing of forest inventory and forest structural features. In this study, the selection of optimal window size, displacement length, and orientation for texture features was guided by the maximization of correlation with forest metrics. Our result showed that moving window size of 35*35 for panchromatic and 9*9 for multispectral image textures had the highest correlation with all three forest metrics. The stronger correlation obtained by larger window sizes can be attributed to the ability of larger window sizes to capture subtle textural differences and variation across larger areas within distinct forest stands (Dye et al., 2008). Alternatively, the poor performance of smaller window sizes might be caused by the fact that smaller window sizes can exaggerate the difference inside the moving window, hence increasing noise in the texture images (Lottering et al., 2020). In terms of displacement length, panchromatic textures displayed the highest association with all forest metrics with a displacement of 1 pixel. This indicates that the panchromatic textures captured the variabilities within the tree crown. The multispectral textures showed the highest correlation with forest metrics calculated with displacement lengths of 2 (3.2 m on the ground) to 5 pixels. The displacement of more than 2 pixels for multispectral textures compared the pixels that were not usually located within the same crown, either between multiple crowns or crown and shadow, given that the forest stands crown diameter range is 3-8m. Moreover, different performances of displacement lengths and window sizes were observed based on the orientations. No specific orientation, but the average orientation showed the highest correlations between multispectral textures and forest metrics. A similar finding was obtained by Kayitakire et al. (2006). They found that the orientation parameter had a marginal effect on estimating forest structure variables in even-aged spruce stands based on IKONOS-2 multispectral imagery. Beguet et al. (2014) found 45-degree orientation of panchromatic texture best correlate with DBH and stand density in a scots pine forest. In our study, we found vertical orientation (90 °) orientation of panchromatic texture best perform for all three forest metrics. The reason for obtaining 90° orientation might be the sun-target-sensor geometry during the image capture. Because of sun's azimuthal angle of 166.8° which was close to 180° and the sensor was in a near-forward position (azimuthal angle = 21.5°), tree shadows were generally projected to the north. Hence, pixels compared in the vertical orientation (90°) were more likely to correspond to tree shadows and illuminated crowns, which had vastly different grey level values.

5.2. Topographic effects in forest metric and image texture relationship

This study examined the changes in the relationship between forest metrics and textural variables by the interaction effects of topographic slope and aspect. However, most of the studies on determining the variability of Norway spruce canopy characteristics found altitude as the most important factor (Pacalaj et al., 2002; Seynave et al., 2011; Socha et al., 2008). We excluded analysing the effect of altitude in our study, since variation in altitude was too small to measure an effect. Our study demonstrates that slope and aspect variation considerably change the relationship between forest metrics and texture characteristics. We found that at steep slopes the relations between texture variables and forest metrics such as Mean DBH and SD DBH became stronger, while the relationship with Tree count became weak. According to Kharuk et al. (2010), at a higher elevation (>1500m) mature forest tend to shift to steep wind protected areas. Similar to slope effect, at higher aspect values (south-facing), panchromatic textures showed stronger relation with Mean and SD DBH, and weaker relation with Tree Count.

5.3. Comparison of model prediction

In the practice of forest structure and growth modelling, region, site quality, topography, and forest management are often regarded essential factors (Justine et al., 2017; Ou et al., 2016). In this study we compared prediction accuracies of forest metrics using models fitted with texture variables and slope, aspect, and their combined interaction effect on texture variables. As indicated in fig. 4.6, incorporation of topographic interaction effect in the model fitted with texture variables, significantly increased the models R^2 and the RMSE was reduced considerably. Our result coincides with the findings of (Ou et al., 2016), though they added slope, elevation, and aspect as independent variable in the model.

For each forest metric, the model having interaction effects of slope and aspect on the texture variable had relatively higher R^2 and lower RMSE compared to the other fitted models. However, AICc values (table 4.4) indicate that combined model was overfitted for Mean DBH and Tree Count. Our results indicate that the Mean DBH and Tree Count models using interaction effects of slope had better model fitting statistics, where SD DBH was better predicted by the effects of combined slope and aspects interaction with texture variables. However, the Mean DBH is better predicted at younger forest and tend to saturate for forest plots with DBH more than 30 cm. Huete et al. (1997) argued that the structure of the NDVI equation, which is a nonlinear transformation of the simple ratio, is the primary cause of nonlinearity and saturation in dense canopy conditions. As an experiment to overcome the problem, we fitted the model for Mean DBH with entropy texture from blue band with slope interaction effect (fig. 5.1) instead of homogeneity from NDVI, which exhibited a reduction in the non-linearity. However, this model resulted in overestimation of Mean DBH at smaller values and underestimation of higher DBH values and obtained lower performance in terms of R^2 , RMSE and AICc values. The comparison of predicted and observed values for SD DBH and Tree Count in fig. 4.7 also exhibited overestimation for smaller values and underestimation at higher values. This is because the even aged forest stands with smooth canopy surface produces higher values of second-order texture (Ozdemir & Karnieli, 2011), thus can be overestimated. On the other hand, trees having larger crowns produces shadow and ground reflections from the canopy gaps yields reduced texture values, thus underestimated the forest metrics at older forest stand.

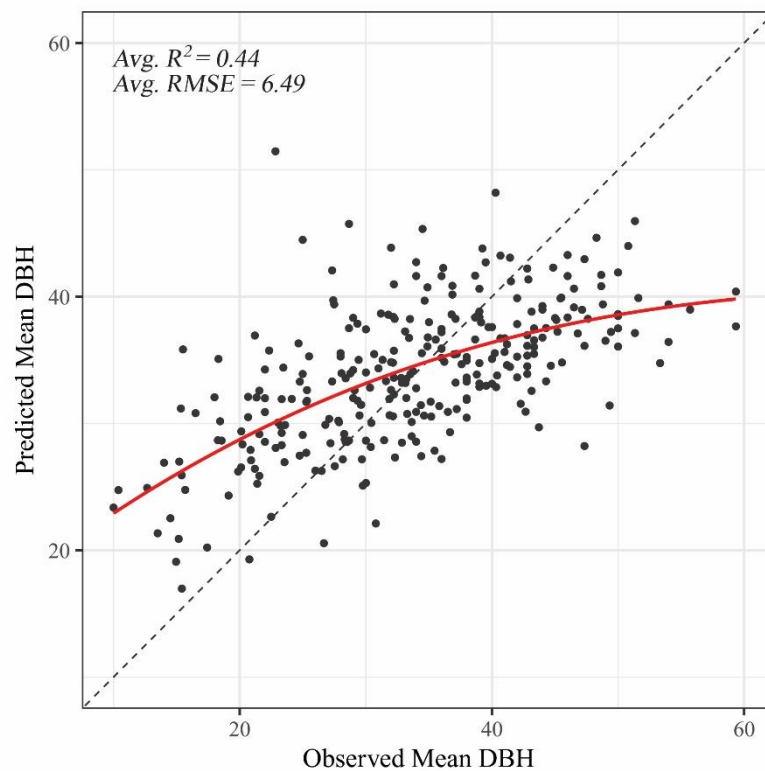


Figure 5. 1: Predicted vs. observed Mean DBH values from the model fitted with panchromatic contrast and blue entropy texture having the interaction effect of slope.

5.4. Prediction of forest metrics influenced by species diversity of stands

Our study findings confirm the initial hypothesis, i.e., “Single species plots produce higher R^2 and lower RMSE than multiple overstory tree species plots from the relationship between Forest stand metrics and remote sensing variables” for Mean DBH and Tree Count. As indicated in table 4.4, the average R^2 was much higher and average RMSE was significantly lower for Mean DBH, and Tree Count models generated using data from plots of single species. This is to be expected because the noise in spectral signature from single-species forest is much lower than the multiple-species stands (Oreti et al., 2021). It is not possible to compare our findings as no previous study was found that compared the estimation of forest inventory data based on species diversity of coniferous forest using multispectral images. However, Heurich & Thoma (2008) using lidar data, found that the estimation error percentage for Mean DBH and Stem density was reduced from 17.9 to 4.9 and 25.3 to 6.3, respectively, when data for the single-species coniferous forest was separated from the mixed forest. We obtained an opposite finding for prediction of SD DBH. The RMSE of SD DBH prediction was significantly lower in multiple species plots. This may be because the contrast texture used to predict SD DBH captured the spectral disparities in multiple species plots more precisely.

6. CONCLUSION AND RECOMMENDATION

6.1. Conclusions

This study aimed to establish a relationship between field-based forest metrics and multispectral remote sensing variables and utilized factors such as slope, aspect and species diversity of forest stands to see if the prediction can further be improved. Several studies included topographic variables as an independent factor in forest structure prediction models but had inconclusive result of whether the topographic variables improved the models. This study investigated the changes in relationship between VHR imagery derived texture variables with forest metrics by the influence of topographic variables. We also compared the forest metrics prediction accuracy in single species conifer stands with multiple species conifer forest stands, which was not investigated before especially with multispectral imagery. On the basis of the presented evidence, we conclude that the answer to the posed research questions would be:

RQ 1: Which image variables correlate significantly (at $\alpha = 0.05$) with forest structural metrics?

The most significantly correlated variable found for Mean DBH was panchromatic contrast with a correlation coefficient of -0.57 and for SD DBH and Tree Count the most significantly correlated variable was correlation from panchromatic band ($r = 0.41$ and -0.56 , respectively). From multispectral textures homogeneity from NDVI, contrast from green band and entropy from blue band was found best correlated variable with Mean DBH, SD DBH and tree Count ($r = -0.47, 0.36$ and -0.51), respectively. Texture variables from panchromatic bands demonstrated the highest correlation when the moving window size was 35×35 , displacement length 1, and a 90° orientation. Texture variables extracted from multispectral bands had the highest correlation when moving window size were 9×9 , displacement 2 to 5, and average direction.

RQ 2: Do the regression coefficients of significant predictor variables change considerably by correcting for slope?

Slope interaction with texture variables significantly changes the relationship of the interacted variable with forest metrics. In most cases, texture variables with interaction effect of slope were the frequently added significant variable in the 100-iteration stepwise model. Incorporating slope as a moderating variable, models' R^2 was improved by 15%, 6%, and 11%, and the RMSE was decreased by 1.03, 0.54, and 0.3 for Mean DBH, SD DBH, and Tree Count, respectively. In the combined models that had an interaction effect of slope and aspect, slope interacted texture variables were most frequently significant for Mean DBH, followed by SD DBH and then Tree Count.

RQ 3: Do the regression coefficients of significant predictor variables change considerably by correcting for aspect?

Aspect interacted texture variables from panchromatic band showed the most frequent significance with Mean DBH and SD DBH. However, textures from the blue band became strongly related with Tree count having an interaction effect of the aspect. Aspect influenced model showed an increased R^2 by 4%, 5%, 5% and RMSE by 0.29, 0.47, 0.17 for Mean DBH, SD DBH, and Tree Count, respectively. Aspect interacted variables became the highest frequent significant variable for SD DBH, when the model variables had combined interaction of slope and aspect.

Finally, Mean DBH, SD DBH and Tree count were predicted with an R^2 of 0.54, 0.45, and 0.42 and RMSE of 6.03, 3.86, and 3.48, respectively, from the best fitted models. Slope had better influence in improvement of estimation accuracy than aspect.

RQ 4: Are the relations between image variables and forest structural metrics stronger (in terms of R^2 and RMSE) in plots with single species than in plots that consist of multiple species?

We observed a stronger relationship between forest metrics (Mean DBH and Tree Count) and texture variables in single species forest stands. However, SD DBH showed stronger relation with texture variables in forest stands having multiple species. Mean DBH and Tree Count is 11% and 8% better explained by texture variables in single species forest. However, SD DBH is 21% better explained by texture variables in multiple species forest stands with a reduction of RMSE from 3.72 to 2.80. Thus, it is evident that diversity on the ground influences image texture capability of predicting forest stand characteristics.

6.2. Potential application and Recommendations for future research

The methods and outcomes presented in this study are intended for forest structure modelling at local scale. The established models and derived relationships may have been applied over a greater area of Rhodope Mountain since the forest structure, composition and topography do not change much in that region. Nevertheless, the variables and coefficients obtained from the models are not likely to be applicable across great distances to other forest ecosystems. Rather, the methods can be followed with new sets of imagery, topographic and field data.

Finally, the following steps are recommended for further development:

- Field survey design: An appropriate plot and sampling design based on the forest stand and topographical characteristics is suggested for more accurate remote sensing-based forest structure estimation. Comparatively smaller plot sizes were employed in this investigation than in previous studies of a similar kind, which may be one of the primary reasons why correlations were lower than in other studies using similar sensor and forest stands.
- As we observed that panchromatic textures with a finer spatial resolution show better correlation with forest metrics than textures from multispectral bands, Pan-sharpening of multispectral bands can be tested for higher correlation. Also, the Pan-sharpening is suggested as fine resolution panchromatic textures showed stronger relations with interaction effects of topography.
- The average orientation (average value of four orientations) used in this study to calculate GLCM textures, should be tested in future studies to document its applicability.
- This study was demonstrated the potential of topographic influence in improvement of prediction accuracy of coniferous forest structural metrics in Rhodope Mountain. However, its applicability in the broadleaf forest needs to be tested. Further study is required to document the interaction effect on texture variables in different environmental condition, including topographic change, species, and forest type.
- Since altitudinal variation highly effect the forest structure, its effect on forest structure estimation improvement should be tested.
- To observe the species diversity influence on forest metric prediction, we used the best fitted models based on topographic influence. Future research might investigate the impact of textures from various spectral bands on differentiating the effect of species diversity on predicting forest structural metrics.

LIST OF REFERENCES

- Aiba, S. I., Takyu, M., & Kitayama, K. (2005). Dynamics, productivity and species richness of tropical rainforests along elevational and edaphic gradients on Mount Kinabalu, Borneo. *Forest Ecosystems and Environments: Scaling Up from Shoot Module to Watershed*, 41–48. https://doi.org/10.1007/4-431-29361-2_4
- AIRBUS. (2020). *WorldDEM™ Technical Product Specification Digital Surface Model, Digital Terrain Model*. <https://earth.esa.int/eogateway/documents/20142/37627/WorldDEM-Technical-Specification.pdf>
- Alin, A. (2010). Multicollinearity. *Wiley Interdisciplinary Reviews: Computational Statistics*, 2(3), 370–374. <https://doi.org/10.1002/WICS.84>
- Avolio, M. L., Pataki, D. E., Gillespie, T. W., Jenerette, G. D., McCarthy, H. R., Pincetl, S., & Clarke, L. W. (2015). Tree diversity in southern California's urban forest: The interacting roles of social and environmental variables. *Frontiers in Ecology and Evolution*, 3(JUL), 73. <https://doi.org/10.3389/FEVO.2015.00073/BIBTEX>
- Babcock, C., Matney, J., Finley, A. O., Weiskittel, A., & Cook, B. D. (2013). Multivariate spatial regression models for predicting individual tree structure variables using LiDAR data. *IEEE Journal of Selected Topics in Applied Earth Observations and Remote Sensing*, 6(1), 6–14. <https://doi.org/10.1109/JSTARS.2012.2215582>
- Baldwin, V. C., Peterson, K. D., Clark, A., Ferguson, R. B., Strub, M. R., & Bower, D. R. (2000). The effects of spacing and thinning on stand and tree characteristics of 38-year-old Loblolly Pine. *Forest Ecology and Management*, 137(1–3), 91–102. [https://doi.org/10.1016/S0378-1127\(99\)00340-0](https://doi.org/10.1016/S0378-1127(99)00340-0)
- Banin, L., Feldpausch, T. R., Phillips, O. L., Baker, T. R., Lloyd, J., Affum-Baffoe, K., Arets, E. J. M. M., Berry, N. J., Bradford, M., Brienen, R. J. W., Davies, S., Drescher, M., Higuchi, N., Hilbert, D. W., Hladik, A., Iida, Y., Salim, K. A., Kassim, A. R., King, D. A., ... Lewis, S. L. (2012). What controls tropical forest architecture? Testing environmental, structural and floristic drivers. *Global Ecology and Biogeography*, 21(12), 1179–1190. <https://doi.org/10.1111/J.1466-8238.2012.00778.X>
- Barbeito, I., Dassot, M., Bayer, D., Collet, C., Drössler, L., Löf, M., del Rio, M., Ruiz-Peinado, R., Forrester, D. I., Bravo-Oviedo, A., & Pretzsch, H. (2017). Terrestrial laser scanning reveals differences in crown structure of *Fagus sylvatica* in mixed vs. pure European forests. *Forest Ecology and Management*, 405, 381–390. <https://doi.org/10.1016/J.FORECO.2017.09.043>
- Baulies, X., & Pons, X. (1995). Approach to forestry inventory and mapping by means of multi-spectral Airborne data. *International Journal of Remote Sensing*, 16(1), 61–80. <https://doi.org/10.1080/01431169508954372>
- Beguet, B., Chehata, N., Boukir, S., & Guyon, D. (2012). Retrieving forest structure variables from Very High Resolution satellite images using an automatic method. *ISPRS Annals of the Photogrammetry, Remote Sensing and Spatial Information Sciences*, 1–2, n.p. <https://doi.org/10.5194/ISPRSANNALS-I-7-1-2012>
- Beguet, B., Guyon, D., Boukir, S., & Chehata, N. (2014). Automated retrieval of forest structure variables based on multi-scale texture analysis of VHR satellite imagery. *ISPRS Journal of Photogrammetry and Remote Sensing*, 96, 164–178. <https://doi.org/10.1016/j.isprsjprs.2014.07.008>
- Behera, M. D., Kushwaha, S. P. S., Dev, M., Ae, B., Prakash, S., & Kushwaha, S. (2006). An analysis of altitudinal behavior of tree species in Subansiri district, Eastern Himalaya. *Biodivers Conserv*, 16, 277–291. https://doi.org/10.1007/978-1-4020-6444-9_18

- Brewer, M. J., Butler, A., & Cooksley, S. L. (2016). The relative performance of AIC, AICC and BIC in the presence of unobserved heterogeneity. *Methods in Ecology and Evolution*, 7(6), 679–692. <https://doi.org/10.1111/2041-210X.12541>
- Brosfoske, K. D., Froese, R. E., Falkowski, M. J., & Banskota, A. (2014). A review of methods for mapping and prediction of inventory attributes for operational forest management. In *Forest Science* (Vol. 60, Issue 4, pp. 733–756). Society of American Foresters. <https://doi.org/10.5849/forsci.12-134>
- Bruniquel-Pinel, V., & Gastellu-Etchegorry, J. P. (1998). Sensitivity of Texture of High Resolution Images of Forest to Biophysical and Acquisition Parameters. *Remote Sensing of Environment*, 65(1), 61–85. [https://doi.org/10.1016/S0034-4257\(98\)00009-1](https://doi.org/10.1016/S0034-4257(98)00009-1)
- Cai, X., & Wang, D. (2006). Spatial autocorrelation of topographic index in catchments. *Journal of Hydrology*, 328(3–4), 581–591. <https://doi.org/10.1016/J.JHYDROL.2006.01.009>
- Castillo-Santiago, M. A., Ricker, M., & de Jong, B. H. J. (2010). Estimation of tropical forest structure from spot-5 satellite images. *International Journal of Remote Sensing*, 31(10), 2767–2782. <https://doi.org/10.1080/01431160903095460>
- Cho, M. A., Skidmore, A. K., & Sobhan, I. (2009). Mapping beech (*Fagus sylvatica* L.) forest structure with airborne hyperspectral imagery. *International Journal of Applied Earth Observation and Geoinformation*, 11(3), 201–211. <https://doi.org/10.1016/J.JAG.2009.01.006>
- Clausi, D. A. (2014). An analysis of co-occurrence texture statistics as a function of grey level quantization. <Http://Dx.Doi.Org/10.5589/M02-004>, 28(1), 45–62. <https://doi.org/10.5589/M02-004>
- Coburn, C. A., & Roberts, A. C. B. (2010). A multiscale texture analysis procedure for improved forest stand classification. <Http://Dx.Doi.Org/10.1080/0143116042000192367>, 25(20), 4287–4308. <https://doi.org/10.1080/0143116042000192367>
- DigitalGlobe. (2010). *DigitalGlobe Core Imagery Products Guide*. <https://www.geosoluciones.cl/documentos/worldview/DigitalGlobe-Core-Imagery-Products-Guide.pdf>
- Donoso, P. J., Soto, D. P., & Bertín, R. A. (2007). Size–density relationships in *Drimys winteri* secondary forests of the Chiloe Island, Chile: Effects of physiography and species composition. *Forest Ecology and Management*, 239(1–3), 120–127. <https://doi.org/10.1016/J.FORECO.2006.11.015>
- Dormann, C. F., Elith, J., Bacher, S., Buchmann, C., Carl, G., Carré, G., Marquéz, J. R. G., Gruber, B., Lafourcade, B., Leitão, P. J., Münkemüller, T., McClean, C., Osborne, P. E., Reineking, B., Schröder, B., Skidmore, A. K., Zurell, D., & Lautenbach, S. (2013). Collinearity: a review of methods to deal with it and a simulation study evaluating their performance. *Ecography*, 36(1), 27–46. <https://doi.org/10.1111/J.1600-0587.2012.07348.X>
- Dupuy, J. M., Hernández-Stefanoni, J. L., Hernández-Juárez, R. A., Tetetla-Rangel, E., López-Martínez, J. O., Leyequién-Abarca, E., Tun-Dzul, F. J., & May-Pat, F. (2012). Patterns and Correlates of Tropical Dry Forest Structure and Composition in a Highly Replicated Chronosequence in Yucatan, Mexico. *Biotropica*, 44(2), 151–162. <https://doi.org/10.1111/J.1744-7429.2011.00783.X>
- Dye, M., Mutanga, O., & Entomology, R. I. (2008). Detecting the severity of woodwasp, *Sirex noctilio*, infestation in a pine plantation in KwaZulu-Natal, South Africa, using texture measures calculated from high spatial. *Journals.Co.Za*, 16(2), 263–275. <https://doi.org/10.4001/1021-3589-16.2.263>

- Eilu, G., & Obua, J. (2005). Proximate composition of wild and on-farm *Tamarindus indica* LINN fruits in the agro-ecological zones of Uganda View project Innovative tools and techniques for sustainable management of the *Vitellaria paradoxa* (the Shea tree) View project. *Tropical Ecology*, 99–111. <https://www.researchgate.net/publication/228960580>
- Ene, L., Næsset, E., & Gobakken, T. (2007). Simulating sampling efficiency in airborne laser scanning based forest inventory. *Int. Arch. Photogram. Remote Sens. Spatial Inf. Sci.*, 36, 114–118. <https://citeseerx.ist.psu.edu/viewdoc/download?doi=10.1.1.221.8759&rep=rep1&type=pdf>
- Fleishman, E., & mac Nally, R. (2006). Patterns of spatial autocorrelation of assemblages of birds, floristics, physiognomy, and primary productivity in the central Great Basin, USA. *Diversity and Distributions*, 12(3), 236–243. <https://doi.org/10.1111/J.1366-9516.2006.00240.X>
- Fortin, M. J., James, P. M. A., MacKenzie, A., Melles, S. J., & Rayfield, B. (2012). Spatial statistics, spatial regression, and graph theory in ecology. *Spatial Statistics*, 1, 100–109. <https://doi.org/10.1016/J.SPASTA.2012.02.004>
- Franklin, S. E., Gerylo, G. R., & Wulder, M. A. (2010a). Texture analysis of IKONOS panchromatic data for Douglas-fir forest age class separability in British Columbia. *Http://Dx.Doi.Org/10.1080/01431160120769*, 22(13), 2627–2632. <https://doi.org/10.1080/01431160120769>
- Franklin, S. E., Gerylo, G. R., & Wulder, M. A. (2010b). Texture analysis of IKONOS panchromatic data for Douglas-fir forest age class separability in British Columbia. *Http://Dx.Doi.Org/10.1080/01431160120769*, 22(13), 2627–2632. <https://doi.org/10.1080/01431160120769>
- Franklin, S. E., Wulder, M. A., & Lavigne, M. B. (1996). Automated derivation of geographic window sizes for use in remote sensing digital image texture analysis. *Computers & Geosciences*, 22(6), 665–673. [https://doi.org/10.1016/0098-3004\(96\)00009-X](https://doi.org/10.1016/0098-3004(96)00009-X)
- Frazer, G. W., Magnussen, S., Wulder, M. A., & Niemann, K. O. (2011). Simulated impact of sample plot size and co-registration error on the accuracy and uncertainty of LiDAR-derived estimates of forest stand biomass. *Remote Sensing of Environment*, 115(2), 636–649. <https://doi.org/10.1016/J.RSE.2010.10.008>
- Freitas, S. R., Mello, M. C. S., & Cruz, C. B. M. (2005). Relationships between forest structure and vegetation indices in Atlantic Rainforest. *Forest Ecology and Management*, 218(1–3), 353–362. <https://doi.org/10.1016/J.FORECO.2005.08.036>
- Fuhr, M., Nasi, R., & Delegue, M. A. (2001). Vegetation structure, floristic composition and growth characteristics of *Aucoumea klaineana* Pierre stands as influenced by stand age and thinning. *Forest Ecology and Management*, 140(2–3), 117–132. [https://doi.org/10.1016/S0378-1127\(00\)00320-0](https://doi.org/10.1016/S0378-1127(00)00320-0)
- Gallardo-Cruz, J. A., Pérez-García, E. A., & Meave, J. A. (2009). β -Diversity and vegetation structure as influenced by slope aspect and altitude in a seasonally dry tropical landscape. *Landscape Ecology*, 24(4), 473–482. <https://doi.org/10.1007/S10980-009-9332-1/FIGURES/5>
- Gamfeldt, L., Snäll, T., Bagchi, R., Jonsson, M., Gustafsson, L., Kjellander, P., Ruiz-Jaen, M. C., Fröberg, M., Stendahl, J., Philipson, C. D., Mikusiński, G., Andersson, E., Westerlund, B., Andrén, H., Moberg, F., Moen, J., & Bengtsson, J. (2013). Higher levels of multiple ecosystem services are found in forests

- with more tree species. *Nature Communications* 2013 4:1, 4(1), 1–8. <https://doi.org/10.1038/ncomms2328>
- Ganault, P., Nahmani, J., Hättenschwiler, S., Gillespie, L. M., David, J. F., Henneron, L., Iorio, E., Mazzia, C., Muys, B., Pasquet, A., Prada-Salcedo, L. D., Wambsganss, J., & Decaëns, T. (2021). Relative importance of tree species richness, tree functional type, and microenvironment for soil macrofauna communities in European forests. *Oecologia*, 196(2), 455–468. <https://doi.org/10.1007/S00442-021-04931-W/FIGURES/2>
- Gobakken, T., & Næsset, E. (2009). Assessing effects of positioning errors and sample plot size on biophysical stand properties derived from airborne laser scanner data. *Http://Doi.Org/10.1139/X09-025*, 39(5), 1036–1052. <https://doi.org/10.1139/X09-025>
- Goff, F. G., & Zedler, P. H. (1968). Structural Gradient Analysis of Upland Forests in the Western Great Lakes Area. *Ecological Monographs*, 38(1), 65–86. <https://doi.org/10.2307/1948537>
- Griffith, D. A. (2013). Establishing Qualitative Geographic Sample Size in the Presence of Spatial Autocorrelation. *Http://Dx.Doi.Org/10.1080/00045608.2013.776884*, 103(5), 1107–1122. <https://doi.org/10.1080/00045608.2013.776884>
- Guisasola, R., Tang, X., Bauhus, J., & Forrester, D. I. (2015). Intra- and inter-specific differences in crown architecture in Chinese subtropical mixed-species forests. *Forest Ecology and Management*, 353, 164–172. <https://doi.org/10.1016/J.FORECO.2015.05.029>
- Hall, R. J., Morton, R. T., & Nesby, R. N. (2011). A Comparison of Existing Models for DBH Estimation from Large-scale Photos. *Http://Doi.Org/10.5558/Tfc65114-2*, 65(2), 114–120. <https://doi.org/10.5558/TFC65114-2>
- Haralick, R. M. (1979). Statistical and structural approaches to texture. *Proceedings of the IEEE*, 67(5), 786–804. <https://doi.org/10.1109/PROC.1979.11328>
- Haralick, R. M., Dinstein, I., & Shanmugam, K. (1973). Textural Features for Image Classification. *IEEE Transactions on Systems, Man and Cybernetics*, SMC-3(6), 610–621. <https://doi.org/10.1109/TSMC.1973.4309314>
- Heineman, K. D., Jensen, E., Shapland, A., Bogenrief, B., Tan, S., Rebarber, R., & Russo, S. E. (2011). The effects of belowground resources on aboveground allometric growth in Bornean tree species. *Forest Ecology and Management*, 261(11), 1820–1832. <https://doi.org/10.1016/J.FORECO.2011.02.005>
- Helmer, E. H., Ruzycki, T. S., Benner, J., Voggesser, S. M., Scobie, B. P., Park, C., Fanning, D. W., & Ramnarine, S. (2012). Detailed maps of tropical forest types are within reach: Forest tree communities for Trinidad and Tobago mapped with multiseason Landsat and multiseason fine-resolution imagery. *Forest Ecology and Management*, 279, 147–166. <https://doi.org/10.1016/J.FORECO.2012.05.016>
- Heurich, M., & Thoma, F. (2008). Estimation of forestry stand parameters using laser scanning data in temperate, structurally rich natural European beech (*Fagus sylvatica*) and Norway spruce (*Picea abies*) forests. *Forestry: An International Journal of Forest Research*, 81(5), 645–661. <https://doi.org/10.1093/FORESTRY/CPN038>
- Holmgren, P., & Thuresson, T. (2008). Satellite remote sensing for forestry planning—A review. *Http://Dx.Doi.Org/10.1080/02827589809382966*, 13(1–4), 90–110. <https://doi.org/10.1080/02827589809382966>

- Houghton, R. A., Lawrence, K. T., Hackler, J. L., & Brown, S. (2001). The spatial distribution of forest biomass in the Brazilian Amazon: a comparison of estimates. *Global Change Biology*, 7(7), 731–746. <https://doi.org/10.1111/J.1365-2486.2001.00426.X>
- Huang, H., Gong, P., Clinton, N., & Hui, F. (2008). Reduction of atmospheric and topographic effect on Landsat TM data for forest classification. <Http://Dx.Doi.Org/10.1080/01431160802082148>, 29(19), 5623–5642. <https://doi.org/10.1080/01431160802082148>
- Huang, H., Li, Z., Gong, P., Cheng, X., Clinton, N., Cao, C., Ni, W., & Wang, L. (2011). Automated methods for measuring DBH and tree heights with a commercial scanning lidar. *Photogrammetric Engineering and Remote Sensing*, 77(3), 219–227. <https://doi.org/10.14358/PERS.77.3.219>
- Huete, A., Jd, W., Leeuwen, V., Huete, A. R., Liu, H., & van Leeuwen, W. J. D. (1997). The use of vegetation indices in forested regions: issues of linearity and saturation. *Ieeexplore.Ieee.Org*. <https://doi.org/10.1109/IGARSS.1997.609169>
- Hyypä, J., Hyypä, H., Inkinen, M., Engdahl, M., Linko, S., & Zhu, Y. H. (2000). Accuracy comparison of various remote sensing data sources in the retrieval of forest stand attributes. *Forest Ecology and Management*, 128(1–2), 109–120. [https://doi.org/10.1016/S0378-1127\(99\)00278-9](https://doi.org/10.1016/S0378-1127(99)00278-9)
- Ingram, J. C., Dawson, T. P., & Whittaker, R. J. (2005). Mapping tropical forest structure in southeastern Madagascar using remote sensing and artificial neural networks. *Remote Sensing of Environment*, 94(4), 491–507. <https://doi.org/10.1016/J.RSE.2004.12.001>
- Johansen, K., & Phinn, S. (2014). Linking riparian vegetation spatial structure in Australian tropical savannas to ecosystem health indicators: semi-variogram analysis of high spatial resolution satellite imagery. <Http://Dx.Doi.Org/10.5589/M06-020>, 32(3), 228–243. <https://doi.org/10.5589/M06-020>
- Jucker, T., Bongalov, B., Burslem, D. F. R. P., Nilus, R., Dalponte, M., Lewis, S. L., Phillips, O. L., Qie, L., & Coomes, D. A. (2018). Topography shapes the structure, composition and function of tropical forest landscapes. *Ecology Letters*, 21(7), 989–1000. <https://doi.org/10.1111/ELE.12964>
- Justine, M. F., Yang, W., Wu, F., & Khan, M. N. (2017). Dynamics of biomass and carbon sequestration across a chronosequence of masson pine plantations. *Journal of Geophysical Research: Biogeosciences*, 122(3), 578–591. <https://doi.org/10.1002/2016JG003619>
- Kane, V. R., Gillespie, A. R., McGaughey, R., Lutz, J. A., Ceder, K., & Franklin, J. F. (2008). Interpretation and topographic compensation of conifer canopy self-shadowing. *Remote Sensing of Environment*, 112(10), 3820–3832. <https://doi.org/10.1016/J.RSE.2008.06.001>
- Karjalainen, M., Kankare, V., Vastaranta, M., Holopainen, M., & Hyypä, J. (2012). Prediction of plot-level forest variables using TerraSAR-X stereo SAR data. *Remote Sensing of Environment*, 117, 338–347. <https://doi.org/10.1016/J.RSE.2011.10.008>
- Kattenborn, T., Hernández, J., Lopatin, J., Kattenborn, G., & Fassnacht, F. E. (2018). PILOT STUDY ON THE RETRIEVAL OF DBH AND DIAMETER DISTRIBUTION OF DECIDUOUS FOREST STANDS USING CAST SHADOWS IN UAV-BASED. <Pdfs.Semanticscholar.Org>. <https://doi.org/10.5194/isprs-annals-IV-1-93-2018>
- Kayitakire, F., Giot, P., & Defourny, P. (2014). Discrimination automatique de peuplements forestiers à partir d'orthophotos numériques couleur: un cas d'étude en Belgique. <Http://Dx.Doi.Org/10.5589/M02-058>, 28(5), 629–640. <https://doi.org/10.5589/M02-058>

- Kayitakire, F., Hamel, C., & Defourny, P. (2006). Retrieving forest structure variables based on image texture analysis and IKONOS-2 imagery. *Remote Sensing of Environment*, 102(3–4), 390–401. <https://doi.org/10.1016/J.RSE.2006.02.022>
- Kharkwal, G., Mehrotra, P., Rawat, Y. S., & Pangtey, Y. P. S. (2005). *Phytodiversity and growth form in relation to altitudinal gradient in the Central Himalayan (Kumaun) region of India*. 89(5), 873–878. <https://www.jstor.org/stable/24111035>
- Kharuk, V. I., Ranson, K. J., Im, S. T., & Vdovin, A. S. (2010). Spatial distribution and temporal dynamics of high-elevation forest stands in southern Siberia. *Global Ecology and Biogeography*, 19(6), 822–830. <https://doi.org/10.1111/J.1466-8238.2010.00555.X>
- Lähde, E., Laiho, O., Norokorpi, Y., & Saksa, T. (1999). Stand structure as the basis of diversity index. *Forest Ecology and Management*, 115(2–3), 213–220. [https://doi.org/10.1016/S0378-1127\(98\)00400-9](https://doi.org/10.1016/S0378-1127(98)00400-9)
- Lamonaca, A., Corona, P., & Barbati, A. (2008). Exploring forest structural complexity by multi-scale segmentation of VHR imagery. *Remote Sensing of Environment*, 112(6), 2839–2849. <https://doi.org/10.1016/J.RSE.2008.01.017>
- Leblanc, S. G. (1998). Applications of the 4-scale radiative-transfer model in the remote sensing of boreal forests. *International Geoscience and Remote Sensing Symposium (IGARSS)*, 3, 1484–1486. <https://doi.org/10.1109/IGARSS.1998.691520>
- Leboeuf, A., Beaudoin, A., Fournier, R. A., Guindon, L., Luther, J. E., & Lambert, M. C. (2007). A shadow fraction method for mapping biomass of northern boreal black spruce forests using QuickBird imagery. *Remote Sensing of Environment*, 110(4), 488–500. <https://doi.org/10.1016/J.RSE.2006.05.025>
- Leitold, V., Michael Keller, Douglas C Morton, Bruce D Cook, & Yosio E Shimabukuro. (2014). Airborne lidar-based estimates of tropical forest structure in complex terrain: Opportunities and trade-offs for REDD+. *Carbon Balance and Management*, 10(1), 1–12. <https://doi.org/10.1186/S13021-015-0013-X/TABLES/3>
- Leuschner, C., Moser, G., Bertsch, C., Röderstein, M., & Hertel, D. (2007). Large altitudinal increase in tree root/shoot ratio in tropical mountain forests of Ecuador. *Basic and Applied Ecology*, 8(3), 219–230. <https://doi.org/10.1016/J.BAAE.2006.02.004>
- Lévesque, J., & King, D. J. (2003). Spatial analysis of radiometric fractions from high-resolution multispectral imagery for modelling individual tree crown and forest canopy structure and health. *Remote Sensing of Environment*, 84(4), 589–602. [https://doi.org/10.1016/S0034-4257\(02\)00182-7](https://doi.org/10.1016/S0034-4257(02)00182-7)
- Liu, Z., Jiang, F., Zhu, Y., Li, F., & Jin, G. (2018). Spatial heterogeneity of leaf area index in a temperate old-growth forest: Spatial autocorrelation dominates over biotic and abiotic factors. *Science of The Total Environment*, 634, 287–295. <https://doi.org/10.1016/J.SCITOTENV.2018.03.333>
- Lottering, R. T., Govender, M., Peerbhay, K., & Lottering, S. (2020). Comparing partial least squares (PLS) discriminant analysis and sparse PLS discriminant analysis in detecting and mapping *Solanum mauritianum* in commercial forest plantations using image texture. *ISPRS Journal of Photogrammetry and Remote Sensing*, 159, 271–280. <https://doi.org/10.1016/J.ISPRSJPRS.2019.11.019>
- Ma, J., Xiao, X., Qin, Y., Chen, B., Hu, Y., Li, X., & Zhao, B. (2017). Estimating aboveground biomass of broadleaf, needleleaf, and mixed forests in Northeastern China through analysis of 25-m ALOS/PALSAR mosaic data. *Forest Ecology and Management*, 389, 199–210. <https://doi.org/10.1016/J.FORECO.2016.12.020>

- Mascaro, J., Detto, M., Asner, G. P., & Muller-Landau, H. C. (2011). Evaluating uncertainty in mapping forest carbon with airborne LiDAR. *Remote Sensing of Environment*, *115*(12), 3770–3774. <https://doi.org/10.1016/J.RSE.2011.07.019>
- Mets, K. D., Armenteras, D., & Dávalos, L. M. (2017). Spatial autocorrelation reduces model precision and predictive power in deforestation analyses. *Ecosphere*, *8*(5), e01824. <https://doi.org/10.1002/ECS2.1824>
- Moisen, G. G., & Frescino, T. S. (2002). Comparing five modelling techniques for predicting forest characteristics. *Ecological Modelling*, *157*(2–3), 209–225. [https://doi.org/10.1016/S0304-3800\(02\)00197-7](https://doi.org/10.1016/S0304-3800(02)00197-7)
- Naesset, E. (2007). Airborne laser scanning as a method in operational forest inventory: Status of accuracy assessments accomplished in Scandinavia. [Http://Dx.Doi.Org/10.1080/02827580701672147](http://Dx.Doi.Org/10.1080/02827580701672147), *22*(5), 433–442. <https://doi.org/10.1080/02827580701672147>
- Næsset, E., Bollandsås, O. M., Gobakken, T., Solberg, S., & McRoberts, R. E. (2015). The effects of field plot size on model-assisted estimation of aboveground biomass change using multitemporal interferometric SAR and airborne laser scanning data. *Remote Sensing of Environment*, *168*, 252–264. <https://doi.org/10.1016/J.RSE.2015.07.002>
- Nikolov, B. P., Zlatanov, T., Groen, T., Stoyanov, S., Hristova-Nikolova, I., & Lexer, M. J. (2022). Habitat requirements of Boreal Owl (*Aegolius funereus*) and Pygmy Owl (*Glaucidium passerinum*) in rear edge montane populations on the Balkan Peninsula. *Avian Research*, *13*, 100020. <https://doi.org/10.1016/J.AVRS.2022.100020>
- Nyamgeroh, B. B., Groen, T. A., Weir, M. J. C., Dimov, P., & Zlatanov, T. (2018). Detection of forest canopy gaps from very high resolution aerial images. *Ecological Indicators*, *95*, 629–636. <https://doi.org/10.1016/J.ECOLIND.2018.08.011>
- Olsson, H. (1994). Changes in satellite-measured reflectances caused by thinning cuttings in Boreal forest. *Remote Sensing of Environment*, *50*(3), 221–230. [https://doi.org/10.1016/0034-4257\(94\)90072-8](https://doi.org/10.1016/0034-4257(94)90072-8)
- Oreti, L., Giuliarelli, D., Tomao, A., & Barbati, A. (2021). Object Oriented Classification for Mapping Mixed and Pure Forest Stands Using Very-High Resolution Imagery. *Remote Sensing 2021, Vol. 13, Page 2508*, *13*(13), 2508. <https://doi.org/10.3390/RS13132508>
- Ou, G., Wang, J., Xu, H., Chen, K., Zheng, H., Zhang, B., Sun, X., Xu, T., & Xiao, Y. (2016). Incorporating topographic factors in nonlinear mixed-effects models for aboveground biomass of natural Simao pine in Yunnan, China. *Journal of Forestry Research*, *27*(1), 119–131. <https://doi.org/10.1007/S11676-015-0143-8>
- Ouma, Y. O., & Tateishi, R. (2006). Optimization of Second-Order Grey-Level Texture in High-Resolution Imagery for Statistical Estimation of Above-Ground Biomass. *Journal of Environmental Informatics*, *8*(2), 70–85. <https://doi.org/10.3808/JEI.200600078>
- Ozdemir, I., & Karnieli, A. (2011). Predicting forest structural parameters using the image texture derived from WorldView-2 multispectral imagery in a dryland forest, Israel. *International Journal of Applied Earth Observation and Geoinformation*, *13*(5), 701–710. <https://doi.org/10.1016/J.JAG.2011.05.006>
- Pacalaj, M., Longauer, R., Krajmerová, D., & Gömöry, D. (2002). Effect of site altitude on the growth and survival of Norway spruce (*Picea abies* L.) provenances on the Slovak plots of IUFRO experiment 1972. *JOURNAL OF FOREST SCIENCE*, *48*(1), 16–26.

- Paoli, G. D., Curran, L. M., & Slik, J. W. F. (2008). Soil nutrients affect spatial patterns of aboveground biomass and emergent tree density in southwestern Borneo. *Oecologia*, *155*(2), 287–299. <https://doi.org/10.1007/S00442-007-0906-9/TABLES/6>
- Park, Y., & Guldmann, J. M. (2020). Measuring continuous landscape patterns with Gray-Level Co-Occurrence Matrix (GLCM) indices: An alternative to patch metrics? *Ecological Indicators*, *109*, 105802. <https://doi.org/10.1016/J.ECOLIND.2019.105802>
- Pasher, J., & King, D. J. (2010). Multivariate forest structure modelling and mapping using high resolution airborne imagery and topographic information. *Remote Sensing of Environment*, *114*(8), 1718–1732. <https://doi.org/10.1016/J.RSE.2010.03.005>
- Pau, S., Gillespie, T. W., & Wolkovich, E. M. (2012). Dissecting NDVI–species richness relationships in Hawaiian dry forests. *Journal of Biogeography*, *39*(9), 1678–1686. <https://doi.org/10.1111/J.1365-2699.2012.02731.X>
- Peddle, D. R., Johnson, R. L., Cihlar, J., & Latifovic, R. (2004). Large area forest classification and biophysical parameter estimation using the 5-Scale canopy reflectance model in Multiple-Forward-Mode. *Remote Sensing of Environment*, *89*(2), 252–263. <https://doi.org/10.1016/J.RSE.2002.08.001>
- Peterson, D. L., Brass, J. A., Westman, W. E., Ambrosia, V. G., Spanner, M. A., & Stephenson, N. J. (1986). Analysis of Forest Structure Using Thematic Mapper Simulator Data. *IEEE Transactions on Geoscience and Remote Sensing*, *GE-24*(1), 113–121. <https://doi.org/10.1109/TGRS.1986.289692>
- Peterson, D. L., Spanner, M. A., Running, S. W., & Teuber, K. B. (1987). Relationship of thematic mapper simulator data to leaf area index of temperate coniferous forests. *Remote Sensing of Environment*, *22*(3), 323–341. [https://doi.org/10.1016/0034-4257\(87\)90087-3](https://doi.org/10.1016/0034-4257(87)90087-3)
- Pierce, K. B., Ohmann, J. L., Wimberly, M. C., Gregory, M. J., & Fried, J. S. (2009). Mapping wildland fuels and forest structure for land management: a comparison of nearest neighbor imputation and other methods. <https://doi.org/10.1139/X09-102>, *39*(10), 1901–1916. <https://doi.org/10.1139/X09-102>
- Pope, G., & Treitz, P. (2013). Leaf Area Index (LAI) Estimation in Boreal Mixedwood Forest of Ontario, Canada Using Light Detection and Ranging (LiDAR) and WorldView-2 Imagery. *Remote Sensing 2013*, *Vol. 5*, Pages 5040-5063, *5*(10), 5040–5063. <https://doi.org/10.3390/RS5105040>
- Pretzsch, H. (2009). Forest Dynamics, Growth, and Yield. *Forest Dynamics, Growth and Yield*, 1–39. https://doi.org/10.1007/978-3-540-88307-4_1
- Pretzsch, H. (2014). Canopy space filling and tree crown morphology in mixed-species stands compared with monocultures. *Forest Ecology and Management*, *327*, 251–264. <https://doi.org/10.1016/J.FORECO.2014.04.027>
- Puhr, C. B., & Donoghue, D. N. M. (2010). Remote sensing of upland conifer plantations using Landsat TM data: A case study from Galloway, south-west Scotland. <https://doi.org/10.1080/014311600210470>, *21*(4), 633–646. <https://doi.org/10.1080/014311600210470>
- Rocha, A. D., Groen, T. A., & Skidmore, A. K. (2019). Spatially-explicit modelling with support of hyperspectral data can improve prediction of plant traits. *Remote Sensing of Environment*, *231*, 111200. <https://doi.org/10.1016/J.RSE.2019.05.019>
- Rock, B. N., Vogelmann, J. E., Williams, D. L., Vogelmann, A. F., & Hoshizaki, T. (1986). Remote Detection of Forest Damage. *BioScience*, *36*(7), 439–445. <https://doi.org/10.2307/1310339>

- Rousset, F., & Ferdy, J. B. (2014). Testing environmental and genetic effects in the presence of spatial autocorrelation. *Ecography*, 37(8), 781–790. <https://doi.org/10.1111/ECOG.00566>
- Ruiz, L. A., Hermosilla, T., Mauro, F., & Godino, M. (2014). Analysis of the Influence of Plot Size and LiDAR Density on Forest Structure Attribute Estimates. *Forests* 2014, Vol. 5, Pages 936-951, 5(5), 936–951. <https://doi.org/10.3390/F5050936>
- Saatchi, S., Houghton, R. A., dos Santos Alvalá, R. C., Soares, J. v., & Yu, Y. (2007). Distribution of aboveground live biomass in the Amazon basin. *Global Change Biology*, 13(4), 816–837. <https://doi.org/10.1111/J.1365-2486.2007.01323.X>
- Sabol, D. E., Gillespie, A. R., Adams, J. B., Smith, M. O., & Tucker, C. J. (2002). Structural stage in Pacific Northwest forests estimated using simple mixing models of multispectral images. *Remote Sensing of Environment*, 80(1), 1–16. [https://doi.org/10.1016/S0034-4257\(01\)00245-0](https://doi.org/10.1016/S0034-4257(01)00245-0)
- Salvador, R., & Pons, X. (1998). On the applicability of Landsat TM images to Mediterranean forest inventories. *Forest Ecology and Management*, 104(1–3), 193–208. [https://doi.org/10.1016/S0378-1127\(97\)00264-8](https://doi.org/10.1016/S0378-1127(97)00264-8)
- Sarker, L. R., & Nichol, J. E. (2011). Improved forest biomass estimates using ALOS AVNIR-2 texture indices. *Remote Sensing of Environment*, 115(4), 968–977. <https://doi.org/10.1016/J.RSE.2010.11.010>
- Scherer-Lorenzen, M., & Schulze, E. (2005). *Forest diversity and function: temperate and boreal systems*. <https://books.google.com/books?hl=en&lr=&id=Dk2ms9cA3OIC&oi=fnd&pg=PA3&ots=WrcK Eijim2&sig=R9hi0VSSNUAk07iVeNOopTQFaRk>
- Scrinzi, G., Marzullo, L., & Galvagni, D. (2007). Development of a neural network model to update forest distribution data for managed alpine stands. *Ecological Modelling*, 206(3–4), 331–346. <https://doi.org/10.1016/J.ECOLMODEL.2007.04.001>
- Seed, E. D., & King, D. J. (2014). Shadow brightness and shadow fraction relations with effective leaf area index: importance of canopy closure and view angle in mixedwood boreal forest. <Http://Dx.Doi.Org/10.5589/M03-003>, 29(3), 324–335. <https://doi.org/10.5589/M03-003>
- Seynave, I., Gégout, J. C., Hervé, J. C., Dhôte, J. F., Drapier, J., Bruno, E., & Dumé, G. (2011). Picea abies site index prediction by environmental factors and understorey vegetation: a two-scale approach based on survey databases. <Https://Doi.Org/10.1139/X05-088>, 35(7), 1669–1678. <https://doi.org/10.1139/X05-088>
- Shannon, C. E. (1948). A Mathematical Theory of Communication. *Bell System Technical Journal*, 27(3), 379–423. <https://doi.org/10.1002/J.1538-7305.1948.TB01338.X>
- Shiklomanov, A. N., Dietze, M. C., Viskari, T., Townsend, P. A., & Serbin, S. P. (2016). Quantifying the influences of spectral resolution on uncertainty in leaf trait estimates through a Bayesian approach to RTM inversion. *Remote Sensing of Environment*, 183, 226–238. <https://doi.org/10.1016/J.RSE.2016.05.023>
- Shugart, H. H., Saatchi, S., & Hall, F. G. (2010). Importance of structure and its measurement in quantifying function of forest ecosystems. *Journal of Geophysical Research: Biogeosciences*, 115(G2), 0–13. <https://doi.org/10.1029/2009JG000993>
- Singh, S., Malik, Z. A., & Sharma, C. M. (2016). Tree species richness, diversity, and regeneration status in different oak (*Quercus* spp.) dominated forests of Garhwal Himalaya, India. *Journal of Asia-Pacific Biodiversity*, 9(3), 293–300. <https://doi.org/10.1016/J.JAPB.2016.06.002>

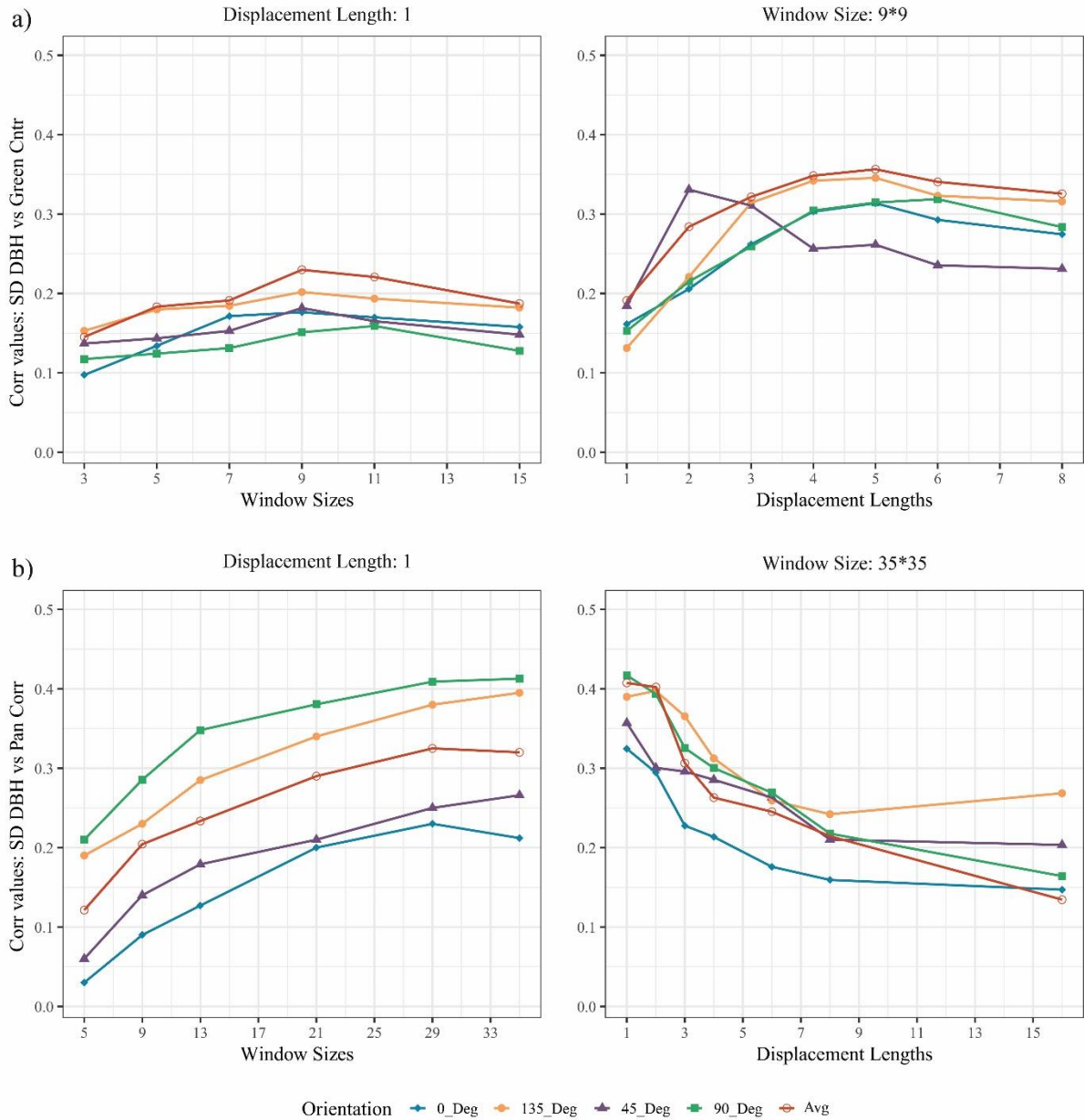
- Socha, J., Carpathian, W., & Jaroslaw Socha, P. (2008). Effect of topography and geology on the site index of *Picea abies* in the West Carpathian, Poland. *Http://Dx.Doi.Org/10.1080/02827580802037901*, 23(3), 203–213. <https://doi.org/10.1080/02827580802037901>
- Solberg, A. H. (1999). Contextual data fusion applied to forest map revision. *IEEE Transactions on Geoscience and Remote Sensing*, 37(3 I), 1234–1243. <https://doi.org/10.1109/36.763280>
- Stellingwerf, D., & Hussin, Y. (1997). *Measurements and estimations of forest stand parameters using remote sensing*. https://books.google.com/books?hl=en&lr=&id=j_-dXK3e7B4C&oi=fnd&pg=PP15&ots=aeyJi5quoJ&sig=0iy3zcyjIsXrl5oRJJ8LYRcK0pQ
- St-Onge, B., Hu, Y., & Vega, C. (2008). Mapping the height and above-ground biomass of a mixed forest using lidar and stereo Ikonos images. *Http://Doi.Org/10.1080/01431160701736505*, 29(5), 1277–1294. <https://doi.org/10.1080/01431160701736505>
- Stoutjesdijk, Ph., & Barkman, J. J. (2014). *Microclimate, vegetation and fauna*. KNNV Publishing. <https://brill.com/view/book/9789004297807/B9789004297807-s001.xml>
- Tan, B., Masek, J. G., Wolfe, R., Gao, F., Huang, C., Vermote, E. F., Sexton, J. O., & Ederer, G. (2013). Improved forest change detection with terrain illumination corrected Landsat images. *Remote Sensing of Environment*, 136, 469–483. <https://doi.org/10.1016/J.RSE.2013.05.013>
- Townsend, P. A. (2002). Estimating forest structure in wetlands using multitemporal SAR. *Remote Sensing of Environment*, 79(2–3), 288–304. [https://doi.org/10.1016/S0034-4257\(01\)00280-2](https://doi.org/10.1016/S0034-4257(01)00280-2)
- Treitz, P., & Howarth, P. (2000). High Spatial Resolution Remote Sensing Data for Forest Ecosystem Classification: An Examination of Spatial Scale. *Remote Sensing of Environment*, 72(3), 268–289. [https://doi.org/10.1016/S0034-4257\(99\)00098-X](https://doi.org/10.1016/S0034-4257(99)00098-X)
- Tuominen, S., & Pekkarinen, A. (2005). Performance of different spectral and textural aerial photograph features in multi-source forest inventory. *Remote Sensing of Environment*, 94(2), 256–268. <https://doi.org/10.1016/J.RSE.2004.10.001>
- Tuttle, E. M., Jensen, R. R., Formica, V. A., & Gonser, R. A. (2006). Using remote sensing image texture to study habitat use patterns: a case study using the polymorphic white-throated sparrow (*Zonotrichia albicollis*). *Global Ecology and Biogeography*, 15(4), 349–357. <https://doi.org/10.1111/J.1466-822X.2006.00232.X>
- Urquiza-Haas, T., Dolman, P. M., & Peres, C. A. (2007). Regional scale variation in forest structure and biomass in the Yucatan Peninsula, Mexico: Effects of forest disturbance. *Forest Ecology and Management*, 247(1–3), 80–90. <https://doi.org/10.1016/J.FORECO.2007.04.015>
- Vázquez De La Cueva, A., Va'zquezva', A., De, V., & Cueva, L. A. (2008). Structural attributes of three forest types in central Spain and Landsat ETM+ information evaluated with redundancy analysis. *Http://Dx.Doi.Org/10.1080/01431160801891853*, 29(19), 5657–5676. <https://doi.org/10.1080/01431160801891853>
- Wang, H., Zhao, Y., Pu, R., & Zhang, Z. (2015). Mapping Robinia Pseudoacacia Forest Health Conditions by Using Combined Spectral, Spatial, and Textural Information Extracted from IKONOS Imagery and Random Forest Classifier. *Remote Sensing 2015, Vol. 7, Pages 9020-9044*, 7(7), 9020–9044. <https://doi.org/10.3390/RS70709020>

- Werner, F. A., & Homeier, J. (2015). Is tropical montane forest heterogeneity promoted by a resource-driven feedback cycle? Evidence from nutrient relations, herbivory and litter decomposition along a topographical gradient. *Functional Ecology*, *29*(3), 430–440. <https://doi.org/10.1111/1365-2435.12351>
- White, J. C., Gómez, C., Wulder, M. A., & Coops, N. C. (2010). Characterizing temperate forest structural and spectral diversity with Hyperion EO-1 data. *Remote Sensing of Environment*, *114*(7), 1576–1589. <https://doi.org/10.1016/J.RSE.2010.02.012>
- Wolter, P. T., Townsend, P. A., & Sturtevant, B. R. (2009). Estimation of forest structural parameters using 5 and 10 meter SPOT-5 satellite data. *Remote Sensing of Environment*, *113*(9), 2019–2036. <https://doi.org/10.1016/J.RSE.2009.05.009>
- Wood, E. M., Pidgeon, A. M., Radeloff, V. C., & Keuler, N. S. (2012). Image texture as a remotely sensed measure of vegetation structure. *Remote Sensing of Environment*, *121*, 516–526. <https://doi.org/10.1016/J.RSE.2012.01.003>
- Wu, J., Yao, W., Choi, S., Park, T., & Myneni, R. B. (2015). A Comparative Study of Predicting DBH and Stem Volume of Individual Trees in a Temperate Forest Using Airborne Waveform LiDAR. *IEEE Geoscience and Remote Sensing Letters*, *12*(11), 2267–2271. <https://doi.org/10.1109/LGRS.2015.2466464>
- Wulder, M. A., Franklin, S. E., Hall, R. J., & Coops, N. C. (2004). High Spatial Resolution Remotely Sensed Data for Ecosystem Characterization. *BioScience*, *54*(6). <https://academic.oup.com/bioscience/article/54/6/511/294008>
- Wulder, M., & Boots, B. (1998). Local spatial autocorrelation characteristics of remotely sensed imagery assessed with the Getis statistic. *International Journal of Remote Sensing*, *19*(11), 2223–2231. <https://doi.org/10.1080/014311698214983>
- Wunderle, A. L., Franklin, S. E., & Guo, X. G. (2007a). Regenerating boreal forest structure estimation using SPOT-5 pansharpened imagery. *International Journal of Remote Sensing*, *28*(19), 4351–4364. <https://doi.org/10.1080/01431160701244849>
- Wunderle, A. L., Franklin, S. E., & Guo, X. G. (2007b). Regenerating boreal forest structure estimation using SPOT-5 pan-sharpened imagery. <https://doi.org/10.1080/01431160701244849>, *28*(19), 4351–4364. <https://doi.org/10.1080/01431160701244849>
- Xie, Y., Zhang, J., Chen, X., Pang, S., Zeng, H., & Shen, Z. (2020). Accuracy assessment and error analysis for diameter at breast height measurement of trees obtained using a novel backpack LiDAR system. *Forest Ecosystems*, *7*(1). <https://doi.org/10.1186/S40663-020-00237-0>
- Yao, W., Krzystek, P., & Heurich, M. (2012). Tree species classification and estimation of stem volume and DBH based on single tree extraction by exploiting airborne full-waveform LiDAR data. *Remote Sensing of Environment*, *123*, 368–380. <https://doi.org/10.1016/J.RSE.2012.03.027>
- Yeakley, J. A., & Weishampel, J. F. (2000). MULTIPLE SOURCE POOLS AND DISPERSAL BARRIERS FOR GALA 'PAGOS GALA 'GALA 'PAGOS PLANT SPECIES DISTRIBUTION. *Reports Ecology*, *81*(4), 893–898. <https://doi.org/10.1890/0012-9658>
- Zach, A., Horna, V., Leuschner, C., & Zimmermann, R. (2010). Patterns of wood carbon dioxide efflux across a 2,000-m elevation transect in an Andean moist forest. *Oecologia*, *162*(1), 127–137. <https://doi.org/10.1007/S00442-009-1438-2/TABLES/4>
- Zenner, E. K., & Hibbs, D. E. (2000). A new method for modeling the heterogeneity of forest structure. *Forest Ecology and Management*, *129*(1–3), 75–87. [https://doi.org/10.1016/S0378-1127\(99\)00140-1](https://doi.org/10.1016/S0378-1127(99)00140-1)

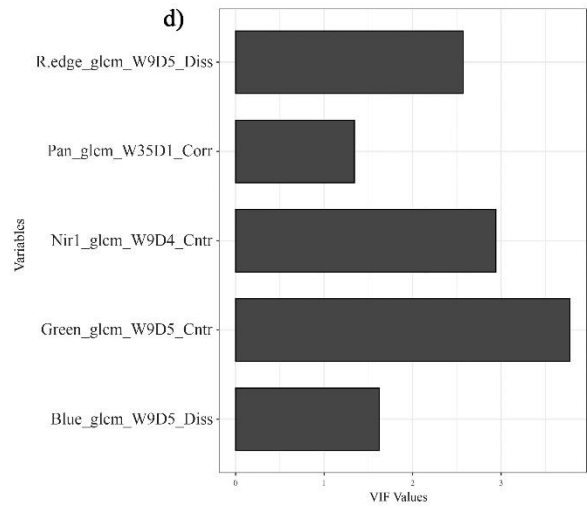
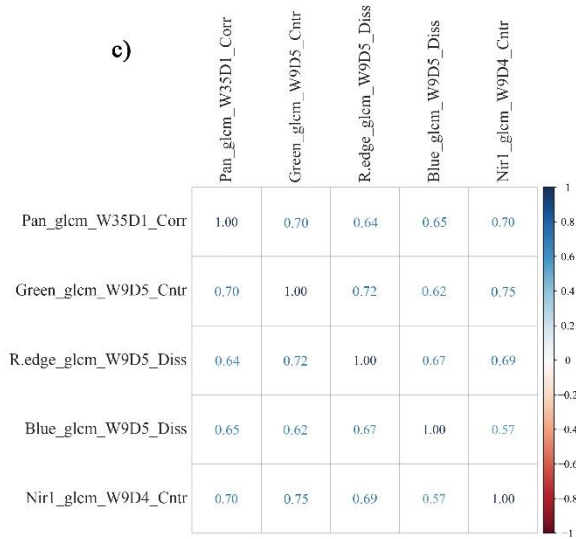
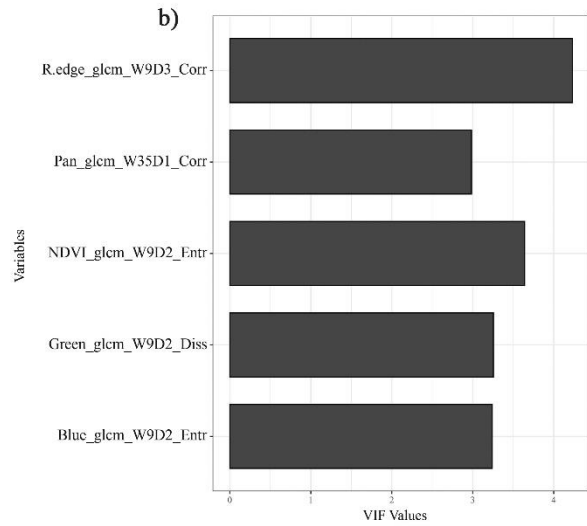
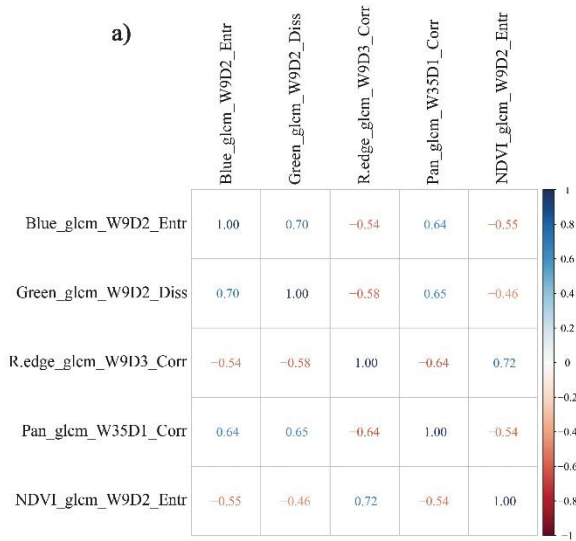
- Zhang, L., Gove, J. H., & Heath, L. S. (2005). Spatial residual analysis of six modeling techniques. *Ecological Modelling*, 186(2), 154–177. <https://doi.org/10.1016/J.ECOLMODEL.2005.01.007>
- Zhao, Q., Wang, F., Zhao, J., Zhou, J., Yu, S., & Zhao, Z. (2018). Estimating Forest Canopy Cover in Black Locust (*Robinia pseudoacacia* L.) Plantations on the Loess Plateau Using Random Forest. *Forests* 2018, Vol. 9, Page 623, 9(10), 623. <https://doi.org/10.3390/F9100623>
- Zhou, J., Yan Guo, R., Sun, M., Di, T. T., Wang, S., Zhai, J., & Zhao, Z. (2017). The Effects of GLCM parameters on LAI estimation using texture values from Quickbird Satellite Imagery. *Scientific Reports* 2017 7:1, 7(1), 1–12. <https://doi.org/10.1038/s41598-017-07951-w>
- Zhou, R., Wu, D., Fang, L., Xu, A., & Lou, X. (2018). A Levenberg–Marquardt Backpropagation Neural Network for Predicting Forest Growing Stock Based on the Least-Squares Equation Fitting Parameters. *Forests* 2018, Vol. 9, Page 757, 9(12), 757. <https://doi.org/10.3390/F9120757>
- Zhou, R., Wu, D., Zhou, R., Fang, L., Zheng, X., & Lou, X. (2019). Estimation of DBH at Forest Stand Level Based on Multi-Parameters and Generalized Regression Neural Network. *Forests* 2019, Vol. 10, Page 778, 10(9), 778. <https://doi.org/10.3390/F10090778>
- Zlatanov, T., Elkin, C., Irauschek, F., & Lexer, M. J. (2017). Impact of climate change on vulnerability of forests and ecosystem service supply in Western Rhodopes Mountains. *Regional Environmental Change*, 17(1), 79–91. <https://doi.org/10.1007/S10113-015-0869-Z/FIGURES/5>

APPENDIX

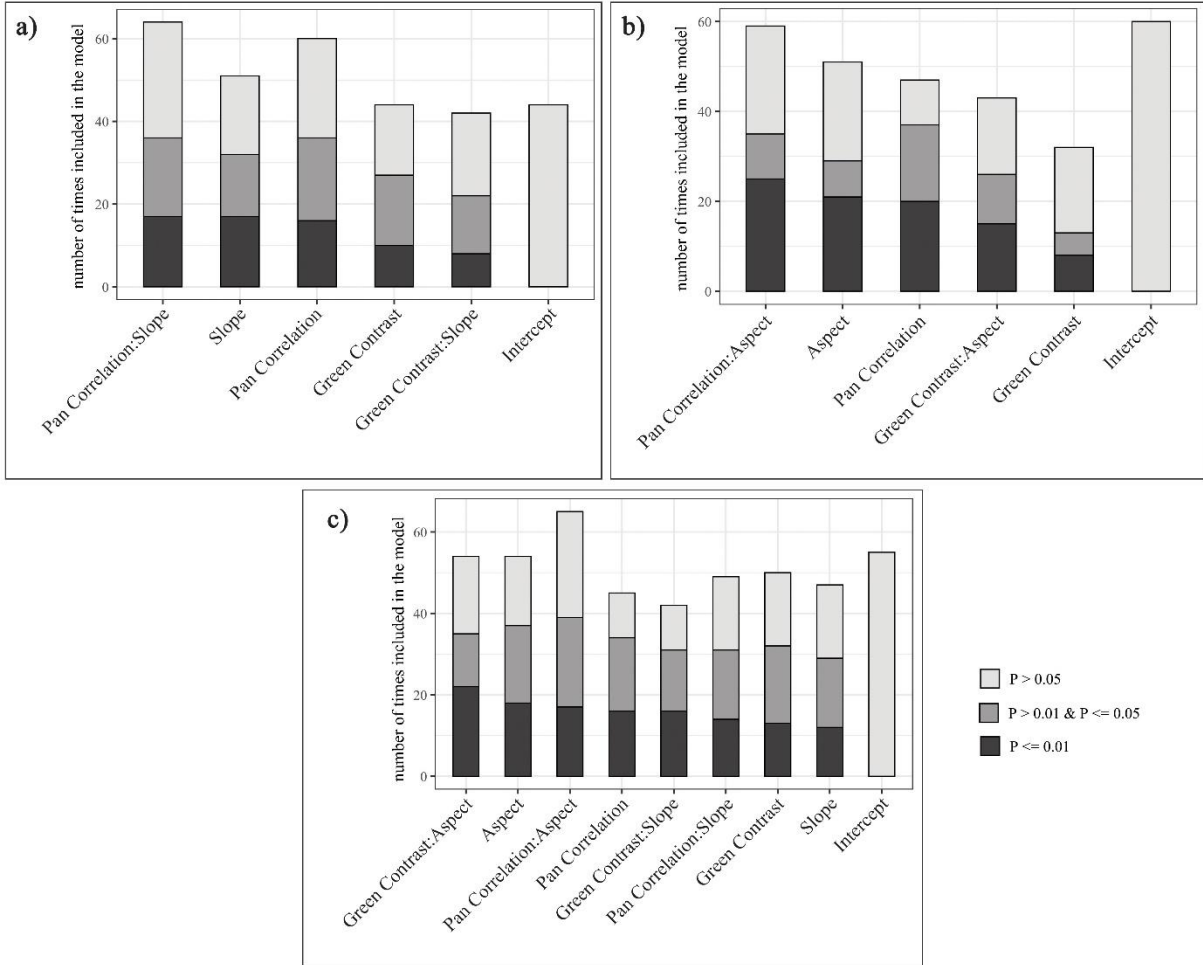
Annex 1: Correlation of texture features with different parameter settings and SD DBH. a) Green Cntr with varying window sizes and displacement length in combination with orientations, b) Pan Corr with varying window sizes and displacement length in combination with orientations.



Annex 2: a) & b) displays the corplot and VIF chart for predictor variables of Tree Count, while c) & d) exhibits the corplot and VIF chart for predictor variables of SD DBH.



Annex 3: Variable significance plot for SD DBH a) Model_{Slope} b) Model_{ASP} c) Model_{Com}, showing the number of times the variables included in the model and became significant at $\alpha = 0.01$ and 0.05.



Annex 4: Variable significance plot for Tree Count a) Model_{Slope} b) Model_{ASP} c) Model_{Com}, showing the number of times the variables included in the model and became significant at $\alpha = 0.01$ and 0.05 .

